Single-Reference ab Initio Methods for the Calculation of Excited States of Large Molecules

Andreas Dreuw*

Institut für Physikalische und Theoretische Chemie, Johann Wolfgang Goethe-Universität, Marie Curie-Strasse 11, 60439 Frankfurt am Main, Germany

Martin Head-Gordon

Department of Chemistry, University of California, and Chemical Sciences Division, Lawrence Berkeley National Laboratory, Berkeley, California 94720-1470

Received April 8, 2005

Contents

1. Introduction

Since the electronic Schrödinger equation (SE) was first written down, it was clear that it cannot be solved exactly for real molecular systems due to the electron−electron interaction and the resulting high dimensionality. Consequently, approximations had to be introduced, which gave birth to the research field of quantum chemistry. The most prominent approximation is the Hartree−Fock approach,[1,2] which treats each electron independently moving in an average field of all other electrons and the nuclei. This leads to an uncoupling of the many-body SE to many single-particle equations, the so-called Hartree−Fock (HF) equations, and concomitantly to the familiar and in chemistry widely used single-particle picture of molecular orbitals. However, an inherent approximation in the HF method is the neglect of electron correlation, that is, the explicit electron−electron interactions. Much effort has been undertaken to recover the missing electron correlation and as a consequence a plethora of quantum chemical ab initio methods have emerged. Examples of such wave-function-based methods are Møller−Plesset perturbation theory (MP),[3,4] configuration interaction (CI),[5,6] and coupled-cluster approaches (CC).[7,8]

A conceptually different approach to include electron correlation is represented by density functional theory (DFT),[9−11] which relies on the electron density as a fundamental quantity. In DFT, exchange and correlation effects are gathered in the so-called exchange−correlation (xc) functional. Since the exact xc functional is unknown, it is fitted empirically to a set of experimental data or it is modeled on the basis of model systems such as the uniform electron gas and other known properties. Once determined, it is then employed as a universal xc functional. Depending on the choice of the ansatz, many different approximate xc functionals are available today. In general, xc functionals can be divided into three different classes: local functionals, gradient-corrected functionals, and hybrid functionals. In fact, the art of performing a DFT calculation is closely related to choosing the appropriate xc functional for the system under investigation. However, DFT is a formally exact theory, that is, if the exact xc functional were used, exact results would be achieved. Density functional theory is built on the famous Hohenberg−Kohn

* E-mail: andreas.dreuw@theochem.uni-frankfurt.de.

10.1021/cr0505627 CCC: $53.50
Published on Web 10/06/2005

Andreas Dreuw was born in 1972 in Neuss, Germany. He received his undergraduate education in chemistry at the universities of Düsseldorf and Heidelberg. In 1997, he joined the theoretical chemistry group of Prof. Lorenz Cederbaum in Heidelberg and received his Ph.D. in 2001. Then he moved to the University of California at Berkeley to join the research group of Prof. Martin Head-Gordon as an "Emmy Noether" postdoctoral fellow of the Deutsche Forschungsgemeinschaft. Since 2003, he has been at the University of Frankfurt where he is leading an independent research group funded within the "Emmy Noether" program. His research interests comprise the development of theoretical methods for the calculation of excited states of large molecules as well as their application to biological problems such as electron and energy transfer processes in phostosynthesis.

Martin Head-Gordon was born in Canberra, Australia (1962), and grew up in Halifax, Canada, and Melbourne, Australia. He received B.Sc. (Hons) and M.Sc. degrees in Chemistry from Monash University, Melbourne, where he worked in the laboratory of Prof. Ron Brown. In 1989, he obtained his Ph.D. in Chemistry from Carnegie-Mellon University, working with Prof. John Pople. After postdoctoral research with Dr. John Tully at Bell Laboratories, Head-Gordon became an Assistant Professor of Chemistry at the University of California, Berkeley, in 1992. He was promoted to Full Professor in 2000, and holds a joint appointment in the Chemical Sciences Division at Lawrence Berkeley National Laboratory. He was a NSF Young Investigator (1993), a Packard Fellow (1995), and a Sloan Fellow (1995), received the Medal of the International Society of Quantum Molecular Sciences (1998), and was a Miller Research Professor (2001–2002). His research centers on the development and application of electronic structure methods and their realization as practical computer algorithms, with particular interests in linear scaling, excited states, and electron correlation.

theorems, HK I and HK II.[12] The first ensures a one-to-one mapping between the electron density and the external potential containing the electron−nuclei attraction and any additional magnetic or electric field, while HK II guarantees the existence of a variational principle for electron densities analogous to the famous Raleigh−Ritz principle for wave functions. Together, HK I and HK II, are the necessary ingredients for the formulation of a many-body theory based on the electron density alone. Present-day DFT calculations are almost exclusively done within the so-called Kohn−Sham formalism,[13] which corresponds to an exact dressed single-particle theory. In analogy to HF theory, the electrons are treated as independent particles moving in the average field of all others but now with correlation included by virtue of the xc functional. This again gives rise to single-electron molecular orbitals and orbital energies. All the methods described so far aim at precise calculation of the electronic ground state of molecular systems, and in principle, they can be divided into wave-function-based methods and density-based methods. Especially Hartree−Fock and DFT form the basis on which excited-state calculations are performed, as we will show in the following paragraphs.

Knowledge about the energetic position of electronically excited states relative to the ground state, as well as information about geometric and electronic properties of excited states, is necessary for the explanation and interpretation of electronic spectra of molecular systems. Furthermore, optically forbidden (dark) states, which are thus experimentally not or only very poorly accessible, very often play important roles in determining the dynamics of electronically excited systems. Quantum chemical calculations of such excited states can, for instance, provide useful information and do indeed often contribute to the fundamental understanding of excited-state dynamics.

Sometimes a ground-state method can be tweaked to calculate a particular electronically excited state, if the ground-state formalism can be forced to converge onto an energetically higher solution by introduction of constraints. These constraints may be given, for example, as a different spin multiplicity; hence one can use a ground state method to calculate the ground state of every possible spin multiplicity. Equally well, the excited state of interest can belong to a different irreducible representation of the spatial symmetry group than the ground state. Then, it is possible to converge the ground-state calculation for the lowest solution of each irreducible representation of the point group of the given molecular system. Following this procedure, excited-state properties such as equilibrium geometries and static electric moments are accessible. The excitation energy is given as the difference of the total energies of the electronic ground state and the excited state obtained in two independent calculations. This method is also commonly referred to as Δ-method. Logically, this methodology breaks down immediately if one is interested in excited states of the same spin multiplicity and same irreducible representation of the spatial symmetry group as the one of the electronic ground state. This is particularly often the case if one seeks to compute optical spectra of large molecular systems, which mostly do not exhibit any spatial symmetry. It is also commonly the case that excited-state configurations are not well represented by the model commonly used for ground-state wave functions, for example open-shell singlets.

Today, several quantum chemical approaches for the calculation of excited states are available that do not require any a priori constraints and that yield energies and oscillator strengths of several excited states in one single calculation. In analogy to ground-state methods, excited-state methods can also be divided into wave-function-based methods and electron-density-based methods. Typical wave-function-based methods are CI,[6,5] multireference CI (MR-CI)[14,15] or multireference MP approaches,[16,17] multiconfigurational self-consistent field (MCSCF) methods,[2] for example, complete active space SCF (CASSCF),[18] and complete active space perturbation theory of second order (CASPT2).[19] These approaches are in principle based on the explicit inclusion of excited states in the many-body wave function as additional so-called "excited" Slater determinants constructed from the HF ground state by swapping occupied with virtual orbitals. The expansion coefficients of the Slater determinants are then calculated via the Raleigh−Ritz variation principle, which in the case of CI corresponds to the diagonalization of the Hamiltonian matrix in the basis of the excited determinants.[1] In multiconfigurational SCF approaches also the expansion coefficients of the molecular orbitals setting up the Slater determinants are reoptimized[1] making these calculations prohibitively computationally expensive for large molecules.

Other prominent wave-function-based approaches are the equation-of-motion[20−22] and linear-response[23−26] coupled cluster theories (EOM-CC and LR-CC, respectively), which depending on the level of truncation in the CC expansion can yield very accurate results. Closely related to these coupled-cluster theories is the symmetry-adapted cluster configuration interaction (SAC-CI) approach.[27] Propagator theories emerging from the Green's function formalism, such as the algebraic diagrammatic construction (ADC) scheme,[28−30] also provide an elegant route to the calculation of excited state properties. However, all these wave-function-based methods are limited to fairly small molecules due to their high computational costs.

The cheapest excited-state methods that include correlation via the wave function available today are the CIS(D) approach[31,32] and the approximate coupled-cluster scheme of second order (CC2).[33,34] The CIS(D) approach is a perturbative correction to configuration interaction singles (CIS)[35] that approximately introduces effects of double excitations for the excited states in a noniterative scheme very similar to MP2, in which doubly excited states are coupled to the ground state. It can also be compared to the perturbative triples correction (T) to the CCSD scheme.[36] Similar in spirit is the CC2 method, which is an approximation to CCSD and of which the linear response functions yield excited states and oscillator strengths of about MP2 quality. CC2 is also closely related to the ADC(2) scheme mentioned before.[37] Modern implementations of these wave-function-based approaches allow for the treatment of molecular systems of up to about 50 atoms.[34]

In this review, we want to focus on single-reference ab initio excited state methods, which are applicable to large molecules and do not explicitly include correlation through the ground-state wave function. In quantum chemical calculations, the size of a molecule is defined by the number of basis functions rather than by the number of atoms, and we are interested in methods that can handle ca. 5000 basis functions in a computation time of maximum a few days on a standard personal computer (PC). If one assumes a typical basis set size of about 15 basis functions per second row atom, one can then investigate molecules with up to 300 such atoms. These restrictions limit the applicable ab initio methods essentially to the wave-function-based methods CIS[35] and time-dependent Hartree−Fock (TDHF), as well as to the density-based approach time-dependent DFT (TDDFT), which builds upon the electron density obtained from ground-state DFT. CIS and TDHF are fairly old methods that have been widely used not only in quantum chemistry but also in nuclear physics, where TDHF is better known as the random phase approximation (RPA) and CIS as the Tamm−Dancoff approximation (TDA) to it.[38] TDDFT, however, is a very modern method that was developed about 20 years ago[39−42] and today has become one of the most prominent methods for the calculation of excited states of medium-sized to large molecules. Several reviews are available in the literature that focus on the theoretical derivation and development of the method,[41−44] but so far, no review focuses on the applicability of TDDFT to various systems, its practical benefits, and its limitations. Also the different available techniques for the analysis of complicated electronic transitions has never been reviewed. The aim of this review is thus threefold. First, CIS, TDHF, and TDDFT are rigorously introduced by outlining their derivations and theoretical footing, where special emphasis is put on their relations to each other. Second, different methods for the analysis of complicated electronically excited states are reviewed and comparatively discussed. Third, we focus on the applicability of the presented methods and show their limitations and point out their strengths and weaknesses.

The review is organized as follows. In the next section (section 2), the wave-function-based methods CIS and TDHF are presented. The derivations and fundamental theoretical concepts are outlined in sections 2.1.1 and 2.2.1 for CIS and TDHF, respectively, and their properties and limitations are discussed in sections 2.1.2 and 2.2.2. Then we turn to time-dependent DFT (section 3), where we first review the theoretical foundations of the theory (section 3.1) and then rederive the basic equations of linear response TDDFT in a density-matrix formulation (section 3.2). The relations between the introduced methods CIS, TDHF, TDDFT/TDA, and TDDFT (section 3.3) and properties and limitations of TDDFT are pointed out (section 3.4). In last subsection 3.5 of this section, we focus on one of the most severe failures of TDDFT for charge-transfer excited states. In section 4, modern schemes for the analysis of electronic transitions are reviewed comprising the analyses of molecular orbitals (section 4.1), the transition density (section 4.2), the difference

density matrix (section 4.3), and attachment/detachment density plots (section 4.4). In the last section 5, two illustrative examples of typical theoretical studies of large molecules employing TDDFT are given, where special emphasis is put onto the applicability, advantages, and limitations of TDDFT.

2. Wave-Function-Based Methods

2.1. Configuration Interaction Singles

2.1.1. Derivation of the CIS Equations

Configuration interaction singles (CIS) is the computationally as well as conceptually simplest wave-function-based ab initio method for the calculation of electronic excitation energies and excited-state properties. The starting point of the derivation of the CIS equations is the Hartree−Fock (HF) ground state, $\Phi_0(r)$, which corresponds to the best single Slater determinant describing the electronic ground state of the system. It reads

$$\Phi_0(r) = |\phi_1(r)\phi_2(r)...\phi_n(r)| \tag{1}$$

For simplicity, we assume a closed-shell ground-state electronic configuration, and thus, the $\phi_i(r)$ correspond to doubly occupied spatial orbitals and $n = N/2$ (N is the number of electrons). $\Phi_0(r)$ is obtained by solving the time-independent Hartree−Fock equation, which is given by

$$\hat{F}(r)\Phi_0(r) = E_0\Phi_0(r) \tag{2}$$

with

$$\hat{F}(r) = \sum_i^n \hat{f}_i(r) \tag{3}$$

and

$$\hat{f}_i(r) = \hat{h}_i(r) + \hat{J}_i(r) - \hat{K}_i(r) \tag{4}$$

In this equation, $\hat{h}(r)$ contains the kinetic energy of the ith electron and its electron−nuclei attraction, while the Coulomb operator $\hat{J}_i(r)$ and exchange operator $\hat{K}_i(r)$ describe the averaged electron−electron interactions. They are defined as

$$\hat{J}_i(r)\phi_i(r) = \left[\sum_j^N \int \mathrm{d}r' \frac{\phi_j^*(r')\phi_j(r')}{|r - r'|}\right]\phi_i(r) \tag{5}$$

$$\hat{K}_i(r)\phi_i(r) = \left[\sum_j^N \int \mathrm{d}r' \frac{\phi_j^*(r')\phi_i(r')}{|r - r'|}\right]\phi_j(r) \tag{6}$$

Solution of the Hartree−Fock equations for the ground-state Slater determinant (eq 1) within a given basis set of size K yields n occupied molecular orbitals, $\phi_i(r)$, and $v = K - n$ virtual orbitals, $\phi_a(r)$. Here and in the following, we use the indices i, j, k, etc. for occupied orbitals, a, b, c, etc. for virtual ones, and p, q, r, etc. for general orbitals. In configuration interaction, the electronic wave function is then constructed as a linear combination of the ground state Slater determinant and so-called "excited" determinants, which are obtained by replacing occupied orbitals of the ground state with virtual ones. If one replaces only one occupied orbital i by one virtual orbital a and one includes only these "singly excited" Slater determinants, $\Phi_i^a(r)$, in the CI wave function expansion, one obtains the CIS wave function, Ψ_{CIS}, which thus reads

$$\Psi_{\mathrm{CIS}} = \sum_{ia} c_i^a \Phi_i^a(r) \tag{7}$$

The summation runs over index pairs ia and has the dimension $n \times v$. This ansatz for the many-body wave function is substituted into the exact time-independent electronic Schrödinger equation,

$$\hat{H}(r)\Psi(r) = [\hat{T}(r) + \hat{V}_{\mathrm{el-nuc}}(r) + \hat{V}_{\mathrm{el-el}}(r)]\Psi(r) = E\Psi(r) \tag{8}$$

where $\hat{T}$ has the usual meaning of the kinetic energy operator

$$\hat{T}(r) = -\sum_i \frac{1}{2}\nabla^2{}_i \tag{9}$$

and $\hat{V}_{\mathrm{el-nuc}}$ corresponds to the electron−nuclei attraction

$$\hat{V}_{\mathrm{el-nuc}}(r) = -\sum_i \sum_K \frac{Z_K}{|r_i - r_K|} \tag{10}$$

where the index i runs over all electrons and K over all nuclei. Z_K is the charge of nucleus K. The electron−electron interaction, $\hat{V}_{\mathrm{el-el}}(r)$ is given as

$$V_{\mathrm{el-el}} = \sum_i^N \sum_{j>i}^N \frac{1}{|r_i - r_j|} \tag{11}$$

Projection onto the space of singly excited determinants, that is, multiplication of eq 8 from the left with $\langle\Phi_j^b|$, yields

$$\sum_{ia}\langle\Phi_j^b|\hat{H}|\Phi_i^a\rangle c_i^a = E_{\mathrm{CIS}}\sum_{ia} c_i^a \delta_{ij}\delta_{ab} \tag{12}$$

and with

$$\langle\Phi_j^b|\hat{H}|\Phi_i^a\rangle = (E_0 + \epsilon_a - \epsilon_i)\delta_{ij}\delta_{ab} + (ia||jb) \tag{13}$$

one readily obtains an expression for the excitation energies $\omega_{\mathrm{CIS}} = E_{\mathrm{CIS}} - E_0$

$$\sum_{ia}\{(\epsilon_a - \epsilon_i)\delta_{ij}\delta_{ab} + (ia||jb)\}c_i^a = \omega_{\mathrm{CIS}}\sum_{ia} c_i^a \delta_{ij}\delta_{ab} \tag{14}$$

ϵ_a and ϵ_i are the orbital energies of the single-electron orbitals ϕ_a and ϕ_i, respectively, and $(ia||jb)$ corre-

sponds to the antisymmetrized two-electron integrals, which are defined as

$$(ia||jb) = \int\int \mathrm{d}r\ \mathrm{d}r' \left[\frac{\phi_i(r)\phi_a(r)\phi_j(r')\phi_b(r') - \phi_i(r)\phi_j(r)\phi_a(r')\phi_b(r')}{|r - r'|}\right] \quad (15)$$

Equation 14 can be nicely written in matrix notation as an eigenvalue equation

$$\mathbf{AX} = \omega\mathbf{X} \quad (16)$$

in which we use the unusual symbol **A** for the matrix representation of the Hamiltonian in the space of the singly excited determinants to make the connection to later occurring equations more clear. ω is the diagonal matrix of the excitation energies, and **X** is the matrix of the CIS expansion coefficients. The matrix elements of **A** are given as

$$A_{ia,jb} = (\epsilon_a - \epsilon_i)\delta_{ij}\delta_{ab} + (ia||jb) \quad (17)$$

The excitation energies are finally obtained by solving the following secular equation

$$(\mathbf{A} - \omega)\mathbf{X} = 0 \quad (18)$$

that is, by diagonalization of the matrix **A**. The obtained eigenvalues correspond to the excitation energies of the excited electronic states, and its eigenvectors to the expansion coefficients according to eq 7.

2.1.2. Properties and Limitations

In the previous section, the derivation of the CIS working equations has been outlined, and it has been shown how excitation energies and excited-state wave functions are obtained. Here, we want to compile some useful properties of CIS:

(1) Since the CIS wave function is determined by variation of the expansion coefficients of the ansatz (eq 7), its total energy corresponds to an upper bound of the true ground-state energy by virtue of the Raleigh−Ritz principle. Also all excited-state total energies are true upper bounds to their exact values. (2) Owing to Brillouin's theorem, which states that "singly excited" determinants $\Phi_i^a(r)$ do not couple to the ground state, that is,

$$\langle\Phi_i^a(r)|\hat{H}|\Phi_0(r)\rangle = 0 \quad (19)$$

the excited state wave functions are Hamiltonian orthogonal to the ground state. (3) In contrast to other truncated configuration interaction methods, for instance, CI with single and double excitations (CISD), CIS is size-consistent, that is, the total ground-state energy of two noninteracting systems is independent of whether they are computed together in one calculation or are computed independently. This is immediately plausible having Brillouin's theorem in mind, owing to which the ground-state energy within CIS is nothing else but the Hartree−Fock energy. And since Hartree−Fock is size-consistent,[1] so is CIS. (4) Another useful property of CIS is that it is possible to obtain pure singlet and triplet states for closed-shell molecules by allowing positive and negative combination of α and β excitations from one doubly occupied orbital. Due to its conceptually simple ansatz (eq 7) and the listed properties, the CIS excited-state wave functions are well defined. Hence, their wave functions and corresponding energies are directly comparable, which is a particularly necessary prerequisite if one is interested in transitions between excited states.

An analytic expression for the total energy of excited states can be obtained from eq 14 by adding E_0 and multiplying from the left with the corresponding CIS vector. It reads

$$E_{\mathrm{CIS}} = E_{\mathrm{HF}} + \sum_{ia}(c_i^a)^2(\epsilon_a - \epsilon_i) + \sum_{ia,jb} c_i^a\, c_j^b(ia||jb) \quad (20)$$

As a consequence, E_{CIS} is analytically differentiable with respect to external parameters, for example, nuclear displacements and external fields, which makes the application of analytic gradient techniques for the calculation of excited-state properties such as equilibrium geometries and vibrational frequencies possible. Analytic first derivatives for CIS excited states have been published,[45,46] and also second derivatives are available.[46] They have been implemented in various computer codes, for instance, Q-Chem, CADPAC, or TURBOMOLE.[47−49]

In general, excitation energies computed with the CIS method are usually overestimated, that is, they are usually too large by about 0.5−2 eV compared with their experimental values (see, for instance, refs 45, 50, and 51). This is on one hand because the "singly excited" determinants derived from the Hartree−Fock ground state are only very poor first-order estimates for the true excitation energies, since the virtual orbital energies ϵ_a are calculated for the $(N + 1)$-electron system instead of for the N-electron system.[1] Consequently, the orbital energy difference $(\epsilon_a - \epsilon_i)$, which is the leading term in eq 17, is not related to an excitation energy, if the canonical Hartree−Fock orbitals are used as reference. In other words, the canonical HF orbitals are not a particularly good basis for the expansion of the correlated wave function, which then needs a high flexibility to compensate for this disadvantage, that is, doubly and higher excited determinants are demanded in the wave function. On the other hand, since electron correlation is generally neglected within the CIS method, the error will be the differential correlation energy, which must be at least on the order of the correlation energy of one and sometimes several electron pairs. Such energies are typically on the order of 1 eV per electron pair, and hence, one should expect errors of this magnitude.

Furthermore, CIS does not obey the Thomas−Reiche−Kuhn dipole sum rule, which states that the sum of transition dipole moments must be equal to the number of electrons.[52−54] Thus, transition moments cannot be expected to be more than qualitatively accurate. While a full presentation of the computational algorithms used to evaluate the CIS energy is beyond our present scope, it is still important to understand the dependence of computational cost on molecule size. The computational cost for CIS

calculations on large molecules is dominated by the evaluation and processing of two-electron integrals in the atomic orbital basis.[45] Per state, this cost scales with the square of the molecule size for sufficiently large systems, because the number of significant two-electron integrals also grows quadratically for large enough molecules (for very small molecules the growth is fourth-order). This is under the assumption that an atomic orbital basis of fixed size (per atom) is chosen. Instead, if the atomic orbital basis on a given atom is increased in size for a given molecule, then the computational cost grows as $O(n^4)$, making large basis set calculations very expensive. This can be reduced to $O(n^3)$ by employing auxiliary basis expansions, as is discussed in section 3.4 for TDDFT. Additionally there are linear algebra operations the cost of which scales with the cube of basis set size that are nonetheless relatively small in comparison to two-electron matrix element contractions.

The small cost of the linear algebra is a result of the use of efficient Davidson-type algorithms[55] to iteratively obtain a small number of excited-state eigenvalues and eigenvectors, in comparison to the very large rank of the CIS matrix, $n(\mathrm{occ}) \times n(\mathrm{virt})$. Direct diagonalization would scale as the cube of this rank, $n(\mathrm{occ})^3 \times n(\mathrm{virt})^3$, which would be with the sixth power of molecule size. Thus iterative diagonalization is critical to the applicability of CIS (and the related TDHF and TDDFT methods) to large molecules. Additionally, iterative diagonalization allows memory requirements to be kept very modest, scaling with the square of system size. This is because the full CIS matrix, **A**, which grows as the square of the rank, $n(\mathrm{occ})^2 \times n(\mathrm{virt})^2$, or the fourth power of molecule size, is never constructed directly. The iterative diagonalization consists of the repeated contraction of the CIS matrix **A** against a trial vector **x** for each state to produce a residual vector **r**. This step in the AO basis becomes the contraction of two-electron integrals with a density-like matrix representing **x**. On today's standard computers, this allows for the treatment of fairly large molecules of about 300 first row atoms or 5000 or so basis functions.

2.2. Time-Dependent Hartree–Fock

The time-dependent Hartree−Fock equations were written down for the first time by Dirac as early as 1930 following a density matrix and equation-of-motion formalism.[56] Since then several different derivations have been given (see, for instance, refs 38 and 57−60), most notably the one by Frenkel using a time-dependent variation principle.[57] The time-dependent Hartree−Fock equations constitute an approximation to the exact time-dependent Schrödinger equation making use of the assumption that the system can at all times be represented by a single Slater determinant composed of time-dependent single-particle wave functions. These equations, however, which will be given later in detail, do not correspond to the scheme that is generally referred to when today's quantum chemists speak of time-dependent Hartree−Fock (TDHF). What is meant, though, are the equations that are obtained in first-order time-dependent perturbation theory from Dirac's equation, that is, the linear response. In the following, we will follow this common convention. In most quantum chemical applications, the TDHF approach is used to calculate electronic excitation spectra and frequency-dependent polarizabilities of molecular systems (for the latter see, for instance, ref 61). Furthermore, the linear response TDHF equations are also well-known in physics under the name random phase approximation (RPA) and have been applied in various fields.[38,59,60]

2.2.1. Concepts and Derivation of TDHF

The starting point of the derivation of the TDHF equation is the general time-dependent electronic Schrödinger equation for molecular systems

$$\hat{H}\Psi(r,t) = i\frac{\partial}{\partial t}\Psi(r,t) \tag{21}$$

where $\hat{H}$ is the time-dependent Hamiltonian

$$\hat{H}(r,t) = \hat{H}(r) + \hat{V}(r,t) \tag{22}$$

where $\hat{H}(r)$ is defined as in eq 8 and $\hat{V}(r,t)$ corresponds to an arbitrary single-particle time-dependent operator, for example, time-dependent electric field

$$\hat{V}(r,t) = \sum_{i}^{N}\hat{v}_i(r,t) \tag{23}$$

With the approximation that $\Psi(r,t)$ can be written as a single Slater determinant (which is the well-known Hartree−Fock assumption) of the form

$$\Phi(r,t) = |\phi_1(r,t)\phi_2(r,t)...\phi_N(r,t)| \tag{24}$$

a time-dependent variant of the Hartree−Fock equation is obtained[56] that reads

$$\hat{F}(r,t)\Phi(r,t) = i\frac{\partial}{\partial t}\Phi(r,t) \tag{25}$$

In addition to the definition of the time-independent Fock operator (eq 3), the operator $\hat{F}(r,t)$ contains the time-dependent single-particle potential $\hat{V}(r,t)$. Furthermore, the Coulomb and exchange operators are analogously defined as in eqs 5 and 6, respectively, but acquire a time dependence since the single-particle wave functions $\phi_i(r,t)$ are now time-dependent.

Let us assume that at $t = 0$ a molecular system is in a stationary state given by a single Slater determinant $\Phi_0(r)$ that obeys the time-independent Hartree−Fock equation (eq 2). Now a small time-dependent perturbation is applied, and the unperturbed orbitals of the Slater determinant will respond to this perturbation but change only slightly, since the perturbation is weak. The TDHF equations are obtained via time-dependent perturbation theory to first order, that is, the linear response of the orbitals and of the time-dependent Fock operator are taken into account. The latter comprises the time-dependent perturbing potential itself as well as the response of the Coulomb and exchange operators due to the change in the orbitals. One possible derivation

of the TDHF equations is via a density matrix formulation, which is outlined later in section 3.2 for TDDFT, and as mentioned earlier, several other routes can be found in the literature (see, for example, refs 2, 38, 59, and 60). Therefore we postpone a detailed derivation until section 3.2. After some algebra and Fourier transformation from the time to the energy domain, one arrives at a non-Hermitian eigenvalue equation, which yields the excitation energies and transition amplitudes as eigenvalues and corresponding eigenvectors. It can be written conveniently in matrix notation as

$$\begin{bmatrix} \mathbf{A} & \mathbf{B} \\ \mathbf{B}^* & \mathbf{A}^* \end{bmatrix} \begin{bmatrix} \mathbf{X} \\ \mathbf{Y} \end{bmatrix} = \omega \begin{bmatrix} 1 & 0 \\ 0 & -1 \end{bmatrix} \begin{bmatrix} \mathbf{X} \\ \mathbf{Y} \end{bmatrix} \tag{26}$$

where the matrix elements are defined as follows

$$A_{ia,jb} = \delta_{ij}\delta_{ab}(\epsilon_a - \epsilon_i) + (ia||jb)$$
$$B_{ia,jb} = (ia||bj) \tag{27}$$

The leading term on the diagonal of the **A** matrix is the difference of the energies of the orbitals i and a, which are the ones from which and to which the electron is excited, respectively. The second term of the **A** matrix and the elements of the **B** matrix, the antisymmetrized two-electron integrals (eq 15), stem from the linear response of the Coulomb and exchange operators to the first-order changes in the single-particle orbitals. It is worthwhile to note, and it will indeed be important later on, that the response of the exchange operator corresponds to a Coulomb-like term and vice versa.

Furthermore, comparison of the TDHF eq 26 with the CIS eigenvalue eq 16 reveals that the latter is contained in the first one: when the **B** matrix of the TDHF equation is set to zero, it reduces to the CIS scheme. In physics, this approximation is well-known as the Tamm−Dancoff approximation,[38,59] which will also be discussed later in section 3.2 in the context of TDDFT. Here, we instantly realize that there exist two different derivation routes to CIS. One is via projection of the Hamiltonian operator $\hat{H}$ onto the space of "singly excited" Slater determinants, a procedure that we will term CI formalism in the following, and the other is by time-dependent response theory to first order and subsequent neglect of the **B** matrix.

2.2.2. Properties and Limitations

In the previous subsection, the basic concepts and the working equation of linear response TDHF has been derived, and it has been shown that it yields excitation energies and transition vectors. In comparison with CIS, TDHF is an extension since it contains not only "singly excited" states but also "singly de-excited" states, which are constructed by interchanging the orbital indices i and a. This statement ought to reflect the attempt to give a mathematical procedure a physical meaning, but of course, the "de-excitations" are nonphysical since one cannot de-excite the Hartree−Fock ground state. Historically one can justify this statement, since TDHF (RPA) has been constructed to include correlation effects in the ground state by virtue of some classes of "doubly excited" Slater determinants, and in this context, one can indeed speak about "de-excited" states.[59] In practice, however, one uses the Hartree−Fock ground state as reference state, and all necessary expectation values are evaluated with respect to it. This approximation is also known as the *quasi-boson approximation*, which in general is reasonable if correlation effects are only small in the corresponding ground state. This again is indicated by the magnitude of the Y amplitudes, which are a measure of the ground-state correlation and which, as a consequence, should be small compared to the X amplitudes.

The time-dependent HF method exhibits similar properties as the CIS scheme. It is a size-consistent method, and one can obtain pure singlet and triplet states for closed-shell molecules. However, TDHF encounters problems with triplet states, and in general, triplet spectra are only very poorly predicted by TDHF calculations. This is because the HF ground state is used as the reference, which in many cases even leads to triplet instabilities.[62] In contrast to CIS, TDHF obeys the Thomas−Reiche−Kuhn sum rule of the oscillator strengths,[63] and thus, one should expect improved transition moments compared to CIS.

It is worthwhile to note that time-dependent HF has a close connection to ground-state HF stability theory, in which it is analyzed whether a converged HF solution is stable in the sense that it corresponds to a minimum in parameter space.[2,62,64] The structure of the equations to be solved for a stability analysis are very similar to the ones for TDHF, and they also contain the first (gradient) and second derivatives (Hessian) of the energy with respect to variational parameters.

Since the energy of the excited states in TDHF are given by an analytical expression that is similar to the one for CIS (eq 20), analytical first derivatives are accessible and have indeed been derived and implemented in connection with TDDFT.[65,66] As we will see later, the analytical derivatives of TDHF are necessary ingredients for analytical gradients in TDDFT when hybrid functionals are employed (section 3.4).

In all applications where the orbitals do not exhibit triplet instabilities, the difference matrix ($\mathbf{A} - \mathbf{B}$, eq 26) becomes positive definite, which allows reduction of the non-Hermitian TDHF eq 26 into a Hermitian eigenvalue equation of half the dimension

$$(\mathbf{A} - \mathbf{B})^{1/2}(\mathbf{A} + \mathbf{B})(\mathbf{A} - \mathbf{B})^{1/2}\mathbf{Z} = \omega^2\mathbf{Z} \tag{28}$$

with

$$\mathbf{Z} = (\mathbf{A} - \mathbf{B})^{-1/2}(\mathbf{X} + \mathbf{Y}) \tag{29}$$

From a technical point of view, the TDHF eq 26 can then in analogy to CIS again be solved using the Davidson procedure,[55] but the computational cost is roughly twice the one of a CIS calculation since in addition to the CIS calculation one has to form trial vector-matrix products also for the **B** matrix.

Although TDHF is in some sense an extension of CIS or equally well CIS is an approximation to

TDHF, TDHF has not been very successful in the quantum chemistry community, that is, it has not been applied very often. Probably, this is because excitation energies calculated with TDHF are slightly smaller than the ones obtained with CIS, but they are still overestimations. The effect of the additional **B** matrix must be only small, since its elements are supposed to be small. Otherwise the underlying "quasi-boson approximation" is a bad one. But if the elements of the **B** matrix are small, one can equally well use the computationally cheaper CIS scheme. More seriously, the problem of the above-mentioned poor treatment of triplet states does not exist in CIS. In summary, TDHF does usually not constitute a significant improvement over CIS that would justify its increased computational cost.

3. Time-Dependent Density Functional Theory

Twenty years after the formulation of the Runge−Gross theorem,[39] which laid the theoretical foundation for time-dependent density functional theory (TDDFT), it has become one of the most prominent and most widely used approaches for the calculation of excited-state properties of medium to large molecular systems, for example, excitation energies, oscillator strengths, excited-state geometries, etc. Every week a large number of publications containing successful applications of TDDFT appear in the literature. In this section, first the formal foundations of TDDFT are reviewed, which comprise the Runge−Gross theorem, the role of the action integral, and the time-dependent Kohn−Sham equation (section 3.1). They represent the necessary ingredients to derive the TDDFT equations in the linear response formulation (section 3.2). Afterward, relations between CIS, TDHF, TDDFT/TDA, and TDDFT are discussed in section 3.3, and properties and limitations of TDDFT are outlined (section 3.4), where special emphasis is put on the failure of TDDFT for CT excited states, which is one of the most severe problems of TDDFT (section 3.5).

3.1. Formal Foundations

Traditional ground-state density functional theory in the Kohn−Sham formulation (KS-DFT) relies on the Hohenberg−Kohn (HK) theorems and the existence of a noninteracting reference system, the electron density of which equals the electron density of the real system (for reviews in the field of ground-state DFT, the reader is referred to refs 9−11, 67, and 68). The first HK theorem (HK I) establishes a one-to-one mapping between the exact electron density, $\rho(r)$, and the exact external potential, $V_{ext}(r)$, and since $V_{ext}(r)$ determines the exact ground-state wave function $\Psi(r)$, the exact ground-state wave function is a functional of the electron density, $\Psi[\rho](r)$. The second HK theorem (HK II) ensures the existence of a variational principle such that the electronic energy of a system calculated with a trial density is always higher than the total energy obtained with the exact density. Both theorems together allow the construction of an exact many-body theory using the electron density as the fundamental quantity. The assumption of the existence of a noninteracting reference system, the ground state of which is a single Slater determinant and the electron density of which is by construction exactly equal to the electron density of the interacting real system, leads to the derivation of the well-known Kohn−Sham (KS) equations.

However, traditional KS-DFT is limited to time-independent systems, that is, ground states, and if one wants to establish an analogous time-dependent theory, time-dependent versions of the first and second HK theorems must be formulated and proven and a time-dependent KS equation must be derived. In the following three subsections, we present the Runge−Gross theorem, which is a time-dependent analogue to HK I, we analyze the role of the action integral in a time-dependent variational principle, and we will outline the derivation of the time-dependent Kohn−Sham equations. The key steps of the mathematical derivations, as well as the associated physical concepts will be outlined.

3.1.1. The Runge–Gross Theorem

The Runge−Gross theorem can be seen as the time-dependent analogue of the first Hohenberg−Kohn theorem and constitutes the cornerstone of the formal foundation of the time-dependent Kohn−Sham formalism.[39] It states that the exact time-dependent electron density, $\rho(r,t)$, determines the time-dependent external potential, $V(r,t)$, up to a spatially constant, time-dependent function $C(t)$ and thus the time-dependent wave function, $\Psi(r,t)$, up to a time-dependent phase factor. The wave function is thus a functional of the electron density

$$\Psi(r,t) = \Psi[\rho(t)](t)\, e^{-i\alpha(t)} \tag{30}$$

with $(d/dt)\alpha(t) = C(t)$. The density, as well as the potential, has to fulfill certain requirements, which we will encounter in detail as we proceed with the proof of the Runge−Gross theorem. The proof starts from the general time-dependent Schrödinger equation

$$i\frac{\partial}{\partial t}\Psi(r,t) = \hat{H}(r,t)\Psi(r,t) \tag{31}$$

where

$$\hat{H}(r,t) = \hat{T}(r) + \hat{V}_{el-el}(r) + \hat{V}_{el-nuc}(r) + \hat{V}(t) \tag{32}$$

$\hat{T}(r)$, $\hat{V}_{el-nuc}$, and $\hat{V}_{el-el}(r)$ correspond to the kinetic energy operator, the electron−nuclei attraction, and electron−electron repulsion as defined in eqs 9−11, respectively. $\hat{V}(t)$ is a time-dependent external potential and is given as a sum of one-particle potentials

$$\hat{V}(t) = \sum_{i}^{N}\hat{v}(r_i,t) \tag{33}$$

N is the number of electrons and is constant with time. The electron density is given as

$$\rho(r,t) = \int |\Psi(r_1,r_2,r_3,...r_N,t)|^2\, dr_2\, dr_3 ... dr_N \tag{34}$$

In the following, spin variables will be omitted for clarity. To prove the Runge−Gross theorem, it must be demonstrated that two densities $\rho^A(r,t)$ and $\rho^B(r,t)$ evolving from a common initial state Ψ_0 under the influence of two different potentials $v^A(r,t)$ and $v^B(r,t)$ are always different if the two potentials differ by more than a purely time-dependent function, that is

$$v^A(r,t) \neq v^B(r,t) + C(t) \tag{35}$$

The first assumption to be made is that the potentials can be expanded in a Taylor series in time around t_0 according to

$$v(r,t) = \sum_{k=0}^{\infty} \frac{1}{k!} \frac{\partial^k v(r,t)}{\partial t^k}|_{t_0}(t-t_0)^k = \sum_{k=0}^{\infty} \frac{1}{k!} v_k(r)(t-t_0)^k \tag{36}$$

Since $v^A(r,t)$ and $v^B(r,t)$ differ by more than a time-dependent function, some of the expansion coefficients, $v_k^A(r) = (\partial^k v^A(r,t))/\partial t^k|_{t_0}$ and $v_k^B(r) = (\partial^k v^B(r,t))/\partial t^k|_{t_0}$, must differ by more than a constant. Hence, there exists one smallest integer k such that

$$v_k^A(r) - v_k^B(r) \neq \text{const} \tag{37}$$

From here, the proof proceeds in two steps. First it will be shown that the current densities, $j^A(r,t)$ and $j^B(r,t)$, corresponding to $v^A(r,t)$ and $v^B(r,t)$ are always different, and in a second step, it will be derived that different current densities require different electron densities. In general, the current density is defined as

$$j(r,t) = \frac{1}{2i}[\Psi^*(r,t)\nabla\Psi(r,t) - \nabla\Psi^*(r,t)\Psi(r,t)] \tag{38}$$

By definition, the current density $j(r,t)$ and the electron density $\rho(r,t)$ obey the so-called continuity equation[69,70]

$$\frac{\partial}{\partial t}\rho(r,t) = -\nabla j(r,t) \tag{39}$$

which states that the temporal change of the electron density in a certain volume is equal to the flux of current density through the surface of that volume. Here, at initial time $t = t_0$, the current densities and the electron densities are given as

$$j^A(r,t_0) = j^B(r,t_0) = j_0(r)$$
$$\rho^A(r,t_0) = \rho^B(r,t_0) = \rho_0(r) \tag{40}$$

and the time-evolution of the current densities $j^A(r,t)$ and $j^B(r,t)$ is given by their equation of motion

$$\frac{\partial}{\partial t}j^A(r,t) = -i\langle\Psi(r,t)|[\hat{j}(r),\hat{H}^A(r,t)]|\Psi(r,t)\rangle$$
$$\frac{\partial}{\partial t}j^B(r,t) = -i\langle\Psi(r,t)|[\hat{j}(r),\hat{H}^B(r,t)]|\Psi(r,t)\rangle \tag{41}$$

Subtraction of these equations yields

$$\frac{\partial}{\partial t}[j^A(r,t) - j^B(r,t)] = -i\langle\Psi(r,t)|[\hat{j}(r),\{\hat{H}^A(r,t) - \hat{H}^B(r,t)\}]|\Psi(r,t)\rangle \tag{42}$$

and evaluation of this expression at $t = t_0$ gives an expression that relates the time evolution of the different current densities to the external potentials. It reads

$$\frac{\partial}{\partial t}[j^A(r,t) - j^B(r,t)]_{t=t_0} = -\rho_0\nabla(v^A(r,t) - v^B(r,t)) \tag{43}$$

Consequently, if the potentials $v^A(r,t)$ and $v^B(r,t)$ differ at $t = t_0$, the right-hand side of eq 43 cannot vanish identically, and hence, the current densities $j^A(r,t)$ and $j^B(r,t)$ will be different infinitesimally later than t_0. Thus we have established a one-to-one mapping between time-dependent potentials and current densities. It is worthwhile to note that eq 43 holds in this form only if eq 36 is satisfied for $k = 0$. If the integer k for which eq 36 holds is greater than zero, the $(k+1)$th time derivative of $(j^A(r,t) - j^B(r,t))$ must be evaluated at $t = t_0$ and the equation of motion is to be applied $(k+1)$ times. Corresponding mathematical expressions can be found, for example, in ref 41, which have a very similar form as eq 43 and lead to the same conclusion. To be able to make this argument, the potential $v(r,t)$ must be expandable in a Taylor expansion in time according to eq 36.

Since now a one-to-one mapping between time-dependent external potentials and time-dependent current densities is established, it remains to be proven that different current densities require different electron densities. For this objective, the continuity equation (eq 39) is applied to $\rho^A(r,t)$ and $\rho^B(r,t)$, and subtraction of the resulting equations and differentiation with respect to time yields

$$\frac{\partial^2}{\partial t^2}[\rho^A(r,t) - \rho^B(r,t)] = -\nabla\frac{\partial}{\partial t}[j^A(r,t) - j^B(r,t)] \tag{44}$$

Insertion of eq 43 yields

$$\frac{\partial^2}{\partial t^2}[\rho^A(r,t) - \rho^B(r,t)] = \nabla[\rho_0\nabla(v^A(r,t) - v^B(r,t))] \tag{45}$$

which corresponds to the desired relation between time-dependent electron densities and time-dependent external potentials. If one can show that the right-hand side of this equation cannot vanish identically, it would be proven that $\rho^A(r,t)$ and $\rho_B(r,t)$ are different if the corresponding external potentials are different. This proof is done by *reductio ad absurdum* assuming that the right-hand side does vanish. According to Gauss' theorem, the following equation is valid

$$\int \rho_0(\nabla(v^A - v^B))^2\, d^3r = -\int (v^A - v^B)\nabla(\rho_0\nabla(v^A - v^B))\, d^3r + \oint (v^A - v^B)\rho_0\nabla(v^A - v^B)\, d\mathbf{S} \tag{46}$$

For real, experimentally realizable potentials, the surface integral vanishes, because the fall off of the asymptote is at least as $1/r$, and the second term of the right-hand side vanishes by assumption. Because the integrand is nonnegative, it follows that for all r

$$\rho_0[\nabla(v^A(r,t) - v^B(r,t))]^2 = 0 \quad (47)$$

and since ρ_0 is greater than zero

$$\nabla(v^A(r,t) - v^B(r,t)) = 0 \quad (48)$$

and thus

$$v^A(r,t) = v^B(r,t) + \text{const} \quad (49)$$

which is in contradiction to the assumption (eq 35). Consequently, the right-hand side of eq 45 cannot vanish identically, and for different time-dependent external potentials at $t = t_0$, one obtains different time-dependent electron densities infinitesimally later than t_0. With this, the one-to-one mapping between time-dependent densities and time-dependent potentials is established, and thus, the potential and the wave function are functionals of the density.

$$\rho(r,t) \leftrightarrow v[\rho](r,t) + C(t) \leftrightarrow \Psi[\rho](r,t)\, e^{-i\alpha(t)}$$

Recently, van Leeuwen presented a generalization of the Runge−Gross theorem and proved that a time-dependent density $\rho(r,t)$ obtained from a many-particle system can under mild restriction on the initial state always be reproduced by an external potential in a many-particle system with *different* two-particle interaction. For two states with equivalent initial state and the same two-particle interaction, van Leeuwen's theorem reduces to the Runge−Gross theorem.[71]

Furthermore, the expectation value of any quantum mechanical operator is a unique functional of the density because the phase factor in the wave function cancels out according to

$$O(t) = \langle \Psi[\rho](r,t)|\hat{O}(t)|\Psi[\rho](r,t)\rangle = O[\rho](t) \quad (50)$$

Strictly speaking, the expectation value implicitly depends also on the initial state, Ψ_0, that is, it is a functional of ρ and Ψ_0. For most cases, however, when Ψ_0 is a nondegenerate ground state, $O[\rho](t)$ is a functional of the density alone, because Ψ_0 is a unique functional of its density ρ_0 by virtue of the traditional first Hohenberg−Kohn theorem.

3.1.2. The Action Integral

In the previous section, the one-to-one mapping between time-dependent potentials and time-dependent functionals has been established, which represents the first step in the development of a time-dependent many-body theory using the density as a fundamental quantity. A second requirement is the existence of a variational principle in analogy to the time-independent case, in which it is given by the above-described second Hohenberg−Kohn theorem. In general, if the time-dependent wave function $\Psi(r,t)$ is a solution of the time-dependent Schrödinger eq 31 with the initial condition

$$\Psi(r,t_0) = \Psi_0(t) \quad (51)$$

then the wave function corresponds to a stationary point of the quantum mechanical action integral.

$$A = \int_{t_0}^{t_1} dt \left\langle \Psi(r,t)\left| i\frac{\partial}{\partial t} - \hat{H}(r,t)\right|\Psi(r,t)\right\rangle \quad (52)$$

which is a functional of $\rho(r,t)$ owing to the above proven Runge−Gross theorem, that is,

$$A[\rho] = \int_{t_0}^{t_1} dt \left\langle \Psi[\rho](r,t)\left| i\frac{\partial}{\partial t} - \hat{H}(r,t)\right|\Psi[\rho](r,t)\right\rangle \quad (53)$$

Consequently, the exact electron density $\rho(r,t)$ can be obtained from the Euler equation

$$\frac{\delta A[\rho]}{\delta \rho(r,t)} = 0 \quad (54)$$

when appropriate boundary conditions are applied. Furthermore from eq 32, the action integral can be split into two parts, one that is universal (for a given number of electrons) and the other dependent on the applied potential $v(r,t) = V_{\text{el-nuc}}(r) + V(r,t)$

$$A[\rho] = B[\rho] - \int_{t_0}^{t_1} dt \int d^3r\, \rho(r,t)v(r,t) \quad (55)$$

The universal functional $B[\rho]$ is independent of the potential $v(r,t)$ and is given as

$$B[\rho] = \int_{t_0}^{t_1} dt \left\langle \Psi[\rho](r,t)\left| i\frac{\partial}{\partial t} - \hat{T}(r) - \hat{V}_{\text{el-el}}(r)\right|\Psi[\rho](r,t)\right\rangle \quad (56)$$

In summary, the variation of the action integral with respect to the density according to eq 54 is a prescription of how the exact density can be obtained. In the next section, this stationary action principle will be applied to derive a time-dependent Kohn−Sham equation in analogy to the time-independent counterpart.

3.1.3. The Time-Dependent Kohn–Sham Equation

In analogy to the derivation of the time-independent Kohn−Sham equations, it is assumed that a time-dependent noninteracting reference system exists with external one-particle potential $v_S(r,t)$ of which the electron density $\rho_S(r,t)$ is equal to the exact electron density $\rho(r,t)$ of the real interacting system. According to the generalization of the Runge−Gross theorem by van Leeuwen,[71] the existence of a time-dependent noninteracting reference system is usually ensured. The noninteracting system is then represented by a single Slater determinant $\Phi(r,t)$ consisting of the single-electron orbitals $\phi_i(r,t)$; thus, its density is given by

$$\rho(r,t) = \rho_S(r,t) = \sum_i^N |\phi_i(r,t)|^2 \quad (57)$$

Provided that the one-particle potential $v_S(r,t)$ exists, the single-electron orbitals are then given as the solution of the time-dependent one-particle Schrödinger equation

$$i\frac{\partial}{\partial t}\phi_i(r,t) = \left(-\frac{1}{2}\nabla_i^2 + v_S(r,t)\right)\phi_i(r,t) \qquad (58)$$

On the other hand, the noninteracting density, which is by assumption equal to the exact density, is also determined by the Euler eq 54, in which the action integral is varied with respect to the density. For the noninteracting system ($\hat{V}_{el-el} = 0$ in eq 56), the action functional takes on the following appearance:

$$A_S[\rho] = B_S[\rho] - \int_{t_0}^{t_1} dt \int d^3r\, \rho(r,t)v_S(r,t) \qquad (59)$$

where

$$B_S[\rho] = \int_{t_0}^{t_1} dt \left\langle \Psi[\rho](r,t)\middle| i\frac{\partial}{\partial t} - \hat{T}(r)\middle|\Psi[\rho](r,t)\right\rangle \qquad (60)$$

and $v(r,t)$ corresponds as usual to the time-dependent external potential as defined in eq 33. Applying the stationary action principle (eq 54) yields

$$\frac{\delta A_S[\rho]}{\delta\rho(r,t)} = 0 = \frac{\delta B_S[\rho]}{\delta\rho(r,t)} - v_S(r,t) \qquad (61)$$

If now a time-dependent single-particle potential $v_S(r,t)$ exists that allows for the construction of the time-dependent single-particle Schrödinger eq 58, this potential is a unique functional of the density by virtue of the Runge−Gross theorem and can according to eq 61 be expressed as

$$v_S(r,t) = \frac{\delta B_S[\rho]}{\delta\xi(r,t)}\Big|_{\xi(r,t)=\rho(r,t)} \qquad (62)$$

evaluated at the exact interacting density $\rho(r,t)$. To obtain more information about the properties of $B_S[\rho]$, one considers the action functional (eq 55) of the interacting system and as a first step rewrites it in the following form

$$A[\rho] = B_S[\rho] - \int_{t_0}^{t_1} dt \int d^3r\, \rho(r,t)v(r,t) - \frac{1}{2}\int_{t_0}^{t_1} dt \int d^3r \int d^3r' \frac{\rho(r,t)\rho(r',t)}{|r-r'|} - A_{xc}[\rho] \qquad (63)$$

A_{xc} is the so-called "exchange−correlation" part of the action integral and is defined as

$$A_{xc}[\rho] = B_S[\rho] - \frac{1}{2}\int_{t_0}^{t_1} dt \int d^3r \int d^3r' \frac{\rho(r,t)\rho(r',t)}{|r-r'|} - B[\rho] \qquad (64)$$

If eq 63 is inserted into the stationary action principle corresponding to the Euler eq 54, one obtains

$$\frac{\delta B_S[\rho]}{\delta\rho(r,t)} = v(r,t) + \int d^3r' \frac{\rho(r',t)}{|r-r'|} + \frac{\delta A_{xc}[\rho]}{\delta\rho(r,t)} \qquad (65)$$

This equation is only solved by the exact interacting density. Comparison with eq 62 gives an expression for the time-dependent single-particle potential

$$v_S(r,t) = v(r,t) + \int d^3r' \frac{\rho(r',t)}{|r-r'|} + \frac{\delta A_{xc}[\rho]}{\delta\rho(r,t)} \qquad (66)$$

Inserting this equation into the time-dependent single-particle Schrödinger eq 58 yields the time-dependent Kohn−Sham equations

$$i\frac{\partial}{\partial t}\phi_i(r,t) = \left(-\frac{1}{2}\nabla_i^2 + v(r,t) + \int d^3r' \frac{\rho(r',t)}{|r-r'|} + \frac{\delta A_{xc}[\rho]}{\delta\rho(r,t)}\right)\phi_i(r,t)$$

$$i\frac{\partial}{\partial t}\phi_i(r,t) = \hat{F}^{KS}\phi_i(r,t) \qquad (67)$$

in which the density is given according to eq 57. The time-dependent Kohn−Sham equations are, in analogy to the time-independent case, single-particle equations in which each electron is treated individually in the field of all others. The kinetic energy of the electrons is represented by $-{}^1/_2\nabla_i^2$; the external time-dependent potential $v(r,t)$ and the Coulomb interaction between the charge distribution of all other electrons with the electron under consideration are explicitly contained. In analogy to the traditional time-independent Kohn−Sham scheme all exchange and correlation effects (explicit Coulomb interaction between the electrons) are collected in $(\delta A_{xc}[\rho])/(\delta\rho(r,t))$. To this end, no approximation has been introduced and consequently the time-dependent Kohn−Sham theory is a formally exact many-body theory. However, the exact time-dependent "exchange−correlation" action functional (also called the xc kernel) is not known, and approximations to this functional have to be introduced. The first approximation generally made is the so-called *adiabatic local density approximation* (ALDA) in which the originally nonlocal (in time) time-dependent xc kernel is replaced with a time-independent local one based on the assumption that the density varies only slowly with time. This approximation allows the use of a standard local ground-state xc potential in the TDDFT framework. The available approximate xc functionals will be discussed in section 3.4.

The time-dependent Kohn−Sham equations can be conveniently expressed in matrix notation in a basis of, say, M time-independent single-particle wave functions $\{\chi_i(r)\}$ such that

$$\phi_p(r,t) = \sum_j^M c_{pj}(t)\chi_j(r) \qquad (68)$$

Then, the time-dependent KS equation reads

$$i\frac{\partial}{\partial t}\mathbf{C} = \mathbf{F}^{KS}\mathbf{C} \qquad (69)$$

Here, the ith column of the matrix $\mathbf{C}$ contains the time-dependent expansion coefficients of $\phi_i(r,t)$ and $\mathbf{F}^{KS}$ is the matrix representation of the time-depend-

ent Kohn−Sham operator in the given basis. Multiplication of eq 69 from the right with $\mathbf{C}^{\dagger}$ and then subtraction from the resultant equation of its Hermitian transpose leads to the Dirac form of the time-dependent Kohn−Sham equation in density matrix form. This equation reads

$$\sum_q \{F_{pq}P_{qr} - P_{pq}F_{qr}\} = i\frac{\partial}{\partial t}P_{pr} \tag{70}$$

in which the density matrix P_{pr} is in general related to the electron density via

$$\begin{aligned}\rho(r,t) &= \sum_{p,q}^{M} c_p(t)c_q^*(t)\chi_p(r)\chi_q^*(r) \\ &= \sum_{p,q}^{M} P_{pq}\chi_p(r)\chi_q^*(r)\end{aligned} \tag{71}$$

To obtain excitation energies and oscillator strengths employing the time-dependent KS approach, two different strategies can be followed. One possibility is to propagate the time-dependent KS wave function in time, which is referred to as real-time TDDFT.[72,73] This technique still has the status of an expert's method but is beginning to be used in chemistry and biophysics, and some successful applications have been reported recently in the literature.[74,75] In the following section, however, we want to focus on the analysis of the linear response of the time-dependent KS equation. This leads to the linear-response TDDFT equations, which correspond to the widely used TDDFT scheme implemented in most standard quantum chemistry codes.

3.2. Derivation of the Linear-Response TDDFT Equation

In this section, the derivation of the linear response TDDFT equation is presented. Using a density matrix formalism, it is shown how the excitation energies are obtained from the linear time-dependent response of the time-independent ground-state electron density to a time-dependent external electric field. Before the time-dependent electric field is applied, the system is assumed to be in its electronic ground state, which is determined by the standard time-independent Kohn−Sham equation, which in the density matrix formulation takes on the following appearance:

$$\sum_q \{F_{pq}^{(0)}\ P_{qr}^{(0)} - P_{pq}^{(0)}\ F_{qr}^{(0)}\} = 0 \tag{72}$$

with the idempotency condition

$$\sum_q P_{pq}^{(0)}\ P_{qr}^{(0)} = P_{pr}^{(0)} \tag{73}$$

$F_{pq}^{(0)}$ and $P_{pq}^{(0)}$ correspond to the Kohn−Sham Hamiltonian and density matrix of the unperturbed ground state, respectively. The elements of the time-independent Kohn−Sham Hamiltonian matrix are given as

$$F_{pq}^{(0)} = \int \mathrm{d}^3r\ \phi_p^*(r)\left\{-\frac{1}{2}\nabla^2 - \sum_{K=1}^{M}\frac{Z_K}{|r-R_K|} + \int \mathrm{d}^3r'\ \frac{\rho(r')}{|r-r'|} + \frac{\delta E_{\mathrm{xc}}}{\delta\rho(r)}\right\}\phi_q(r) \tag{74}$$

In the basis of the orthonormal unperturbed single-particle orbitals of the ground state, these matrices are simply given as

$$F_{pq}^{(0)} = \delta_{pq}\epsilon_p \tag{75}$$

and

$$\begin{aligned}P_{ij}^{(0)} &= \delta_{ij} \\ P_{ia}^{(0)} = P_{ai}^{(0)} &= P_{ab}^{(0)} = 0\end{aligned} \tag{76}$$

Again, we follow the convention that indices i, j, etc. correspond to occupied orbitals, a, b, etc. correspond to virtual orbitals and p, q, r, etc. refer to general orbitals, and ϵ_p is the orbital energy of the one-electron orbital p.

Now, an oscillatory time-dependent external field is applied, and the first-order (linear) response to this perturbation is analyzed. In general perturbation theory, the wave function or in this case the density matrix is assumed to be the sum of the unperturbed ground state and its first-order time-dependent change,

$$P_{pq} = P_{pq}^{(0)} + P_{pq}^{(1)} \tag{77}$$

The same holds for the time-dependent Kohn−Sham Hamiltonian, which to first order is given as the sum of the ground-state KS Hamiltonian and the first-order change

$$F_{pq} = F_{pq}^{(0)} + F_{pq}^{(1)} \tag{78}$$

Substituting eqs 77 and 78 into the time-dependent Kohn−Sham eq 70 and collecting all terms of first order yield

$$\sum_q [F_{pq}^{(0)}\ P_{qr}^{(1)} - P_{pq}^{(1)}\ F_{qr}^{(0)} + F_{pq}^{(1)}\ P_{qr}^{(0)} - P_{pq}^{(0)}\ F_{qr}^{(1)}] = i\frac{\partial}{\partial t}P_{pr}^{(1)} \tag{79}$$

The first-order change of the Kohn−Sham Hamiltonian consists of two terms. The first contribution corresponds to the applied perturbation, the time-dependent electric field itself, and it has been shown that it is sufficient to consider only a single Fourier component of the perturbation,[2] which is given in matrix notation as

$$g_{pq} = \frac{1}{2}[f_{pq}\,\mathrm{e}^{-i\omega t} + f_{qp}^*\,\mathrm{e}^{i\omega t}] \tag{80}$$

In this equation, the matrix f_{pq} is a one-electron operator and describes the details of the applied perturbation. Furthermore, the two-electron part of the Kohn−Sham Hamiltonian reacts on the changes in the density matrix, on which it explicitly depends. The changes in the KS Hamiltonian due to the change of the density are given to first order as

$$\Delta F_{pq}^{(0)} = \sum_{st} \frac{\partial F_{pq}^{(0)}}{\partial P_{st}} P_{st}^{(1)} \tag{81}$$

such that the first-order change in the KS Hamiltonian is altogether given as

$$F_{pq}^{(1)} = g_{pq} + \Delta F_{pq}^{(0)} \tag{82}$$

Turning to the time-dependent change of the density matrix induced by the perturbation of the KS Hamiltonian, this is to first order given as

$$P_{pq}^{(1)} = \frac{1}{2}[d_{pq}\, e^{-i\omega t} + d_{qp}^{*}\, e^{i\omega t}] \tag{83}$$

where d_{pq} represent perturbation densities. Inserting eqs 80−83 into eq 79 and collecting the terms that are multiplied by $e^{-i\omega t}$ yield the following expression

$$\sum_{q}\left[F_{pq}^{(0)}d_{qr} - d_{pq}F_{qr}^{(0)} + \left(f_{pq} + \sum_{st}\frac{\partial F_{pq}^{(0)}}{\partial P_{st}} d_{st}\right)P_{qr}^{(0)} - P_{pq}^{(0)}\left(f_{qr} + \sum_{st}\frac{\partial F_{qr}^{(0)}}{\partial P_{st}} d_{st}\right)\right] = \omega d_{pr} \tag{84}$$

The terms multiplied by $e^{i\omega t}$ lead to the complex conjugate of the above equation. The idempotency condition (eq 73) gives an expression for the first-order change of the density matrix of the form

$$\sum_{q}\{P_{pq}^{(0)}P_{qr}^{(1)} + P_{pq}^{(1)}P_{qr}^{(0)}\} = P_{pr}^{(1)} \tag{85}$$

which restricts the form of the matrix d_{pq} in eq 84 such that occupied−occupied and virtual−virtual blocks d_{ii} and d_{aa} are zero, and only the occupied−virtual and virtual−occupied blocks, d_{ia} and d_{ai}, respectively, contribute and are taken into account. Remembering the diagonal nature of the unperturbed KS Hamiltonian and density matrixes, one obtains the following pair of equations:

$$F_{aa}^{(0)}x_{ai} - x_{ai}F_{ii}^{(0)} + \left(f_{ai} + \sum_{bj}\left\{\frac{\partial F_{ai}}{\partial P_{bj}}x_{bj} + \frac{\partial F_{ai}}{\partial P_{jb}}y_{bj}\right\}\right)P_{ii}^{(0)} = \omega x_{ai} \tag{86}$$

$$F_{ii}^{(0)}y_{ai} - y_{ai}F_{aa}^{(0)} - P_{ii}^{(0)}\left(f_{ia} + \sum_{bj}\left\{\frac{\partial F_{ia}}{\partial P_{bj}}x_{bj} + \frac{\partial F_{ia}}{\partial P_{jb}}y_{bj}\right\}\right) = \omega y_{ai} \tag{87}$$

where we have set $x_{ai} = d_{ai}$ and $y_{ai} = d_{ia}$ to follow conventional nomenclature. In the zero-frequency limit ($f_{ai} = f_{ia} = 0$), that is, under the assumption that the electronic transitions occur for an infinitesimal perturbation, and making use of the fact that in the basis of the canonical orbitals $F_{pp}^{(0)} = \epsilon_p$ and $P_{ii}^{(0)} = 1$ (eqs 75 and 76), one obtains a non-Hermitian eigenvalue equation, the TDDFT equation,

$$\begin{bmatrix}\mathbf{A} & \mathbf{B}\\ \mathbf{B}^{*} & \mathbf{A}^{*}\end{bmatrix}\begin{bmatrix}\mathbf{X}\\ \mathbf{Y}\end{bmatrix} = \omega\begin{bmatrix}1 & 0\\ 0 & -1\end{bmatrix}\begin{bmatrix}\mathbf{X}\\ \mathbf{Y}\end{bmatrix} \tag{88}$$

the structure of which is equivalent to the TDHF eq 26 introduced in section 2.2. Here, the elements of the matrices **A** and **B** are given as

$$A_{ia,jb} = \delta_{ij}\delta_{ab}(\epsilon_a - \epsilon_i) + (ia|jb) + (ia|f_{xc}|jb)$$
$$B_{ia,jb} = (ia|bj) + (ia|f_{xc}|bj) \tag{89}$$

where the two-electron integrals are again given in Mulliken notation. In comparison with the TDHF eq 26, the definitions of the matrix elements differ only in their last terms. While in TDHF the last terms correspond to the response of the nonlocal HF exchange potential, which yields a Coulomb-like term, they correspond in TDDFT to the response of the chosen xc potential, which replaces the HF exchange potential in KS-DFT. In the ALDA approximation (see section 3.1.3), the response of the xc potential corresponds to the second functional derivative of the exchange−correlation energy, which is also called the xc kernel, and is given as

$$(ia|f_{xc}|jb) = \int d^3r\, d^3r'\, \phi_i^{*}(r)\phi_a(r)\frac{\delta^2 E_{xc}}{\delta\rho(r)\delta\rho(r')}\phi_b^{*}(r')\phi_j(r') \tag{90}$$

Explicit expressions for the xc kernel are given, for example, in ref 76.

An alternative elegant route to the derivation of the linear response expressions for TDDFT (eq 88) via the energy-dependent density−density response function $\chi(r,r',\omega)$ of the interacting system, which contains all physical information about how the exact density $\rho(r,\omega)$ changes upon small changes in the external potential $v_{ext}(r,\omega)$, has been presented by Marques and Gross.[44] The quantities are energy-dependent since they correspond to the Fourier transforms of the corresponding time-dependent ones. The change in the density can equally well be calculated using the response of the noninteracting Kohn−Sham system, $\chi_{KS}(r,r',\omega)$ and is given as

$$\delta\rho(r,\omega) = \int d^3r'\, \chi_{KS}(r,r',\omega)\delta v_S(r',\omega) \tag{91}$$

From eq 91 a formally exact expression for the exact density response function of the interacting system can be derived that reads

$$\chi(r,r',\omega) = \chi_{KS}(r,r',\omega) + \int d^3r'' \int d^3r'''\, \chi(r,r'',\omega)\left[\frac{1}{|r''-r'''|} + f_{xc}(r'',r''',\omega)\right]\chi_{KS}(r''',r',\omega) \tag{92}$$

Knowing that the exact density response function possesses poles at the exact excitation energies of the system,[44] one can starting from eq 92 through a series

of algebraic manipulations arrive at a pseudo-eigenvalue equation similar to eq 88, which yields exact excitation energies. If furthermore the single-pole approximation (SPA)[77] and the ALDA approximation as described in section 3.1.3 are employed, one obtains exactly the linear-response TDDFT, eq 88.

In analogy to TDHF and CIS (section 2.2), the Tamm−Dancoff approximation (TDA) to TDDFT has recently been introduced.[78] Again, it corresponds to neglecting the matrix **B** in eq 88, that is, only the occupied−virtual block of the initial **d** matrix (eq 84) is taken into account. This leads to a Hermitian eigenvalue equation

$$\mathbf{AX} = \omega\mathbf{X} \tag{93}$$

where the definition of the matrix elements of **A** is still the same as in eq 89. It is worthwhile to note that TDA/TDDFT is usually a very good approximation to TDDFT.[78,79] A possible reason may be that in DFT correlation is already included in the ground state by virtue of the xc functional, which is not the case in HF theory. Since the magnitude of the **Y** amplitudes and the elements of the **B** matrix are a measure for missing correlation in the ground state, they should be even smaller in TDDFT than in TDHF and, thus, be less important. TDDFT is also more resistant to triplet instabilities than TDHF.

Equations 88 and 89 represent the TDDFT formalism, which is solved to obtain excitation energies ω and transition vectors $|XY\rangle$ when the unperturbed KS Hamiltonian (eq 74), from which the response is derived, contains a so-called pure DFT xc potential and not also parts of Hartree−Fock exchange. However, today it is very common to include parts of Hartree−Fock exchange in the xc potential, which corresponds to using so-called hybrid functionals. For instance, the widely used B3LYP functional contains 20% HF exchange ($c_{\mathrm{HF}} = 0.2$ in eq 94).[80] In this case, the unperturbed KS Hamiltonian acquires an additional term and takes on the following appearance:

$$F_{pq}^{(0)} = \int \mathrm{d}^3 r\, \phi_p^*(r)\Bigg\{-\frac{1}{2}\nabla^2 + \sum_{K=1}^{M}\frac{-Z_K}{|r-R_K|} + \int \mathrm{d}^3 r' \frac{\rho(r')}{|r-r'|} - c_{\mathrm{HF}}\int \mathrm{d}^3\, r' \frac{\rho(r,r')}{|r-r'|} + (1-c_{\mathrm{HF}})\frac{\delta E_{\mathrm{xc}}}{\delta\rho(r)}\Bigg\}\phi_q(r) \tag{94}$$

Using this more general time-independent KS Hamiltonian and following the same derivation route as above, one arrives at more general expressions for the TDDFT equations, which allow for the use of hybrid functionals. Although the non-Hermitian eigenvalue eq 88 remains the same, the elements of its matrices **A** and **B** are now given as

$$A_{ia,jb} = \delta_{ij}\delta_{ab}(\epsilon_a - \epsilon_i) + (ia|jb) - c_{\mathrm{HF}}(ij|ab) + (1-c_{\mathrm{HF}})(ia|f_{\mathrm{xc}}|jb) \tag{95}$$

$$B_{ia,jb} = (ia|bj) - c_{\mathrm{HF}}(ib|aj) + (1-c_{\mathrm{HF}})(ia|f_{\mathrm{xc}}|bj) \tag{96}$$

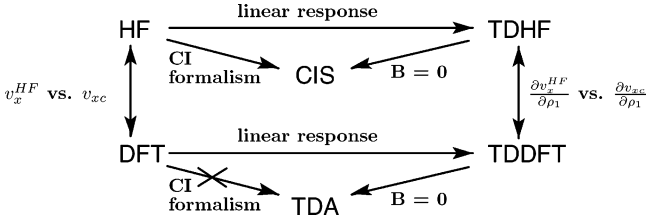

Figure 1. Schematic sketch of the relation between Hartree−Fock (HF) and density functional theory (DFT), time-dependent Hartree−Fock and time-dependent DFT (TDDFT), and configuration interaction singles (CIS) and the Tamm−Dancoff approximation to TDDFT (TDA).

containing the response of the Hartree−Fock exchange potential, as well as the one of the chosen xc potential at a rate determined by the factor c_{HF} determined in the hybrid xc functional. Comparing the definitions of the matrix elements of TDHF (eqs 27) and TDDFT (eqs 89) with eq 96, it becomes apparent that the latter equation contains TDHF and TDDFT as limiting cases if $c_{\mathrm{HF}} = 1$ or $c_{\mathrm{HF}} = 0$, respectively. In other words, eq 96 corresponds to a linear combination of eqs 27 and 89 thereby combining TDHF and TDDFT in one hybrid scheme.

3.3. Relation of TDDFT and TDHF, TDDFT/TDA, and CIS

In the previous section, we have seen that TDDFT and TDHF are closely related by a hybrid scheme that emerges when the unperturbed Kohn−Sham Hamiltonian contains both a nonlocal Hartree−Fock exchange potential and a local xc potential. In Figure 1, the relations between the introduced methods CIS and TDHF as well as TDDFT/TDA and TDDFT are schematically shown. Starting from the usual time-independent Hartree−Fock scheme, the ground-state Kohn−Sham equations are in principle obtained by exchanging the nonlocal HF exchange potential, $v_{\mathrm{x}}^{\mathrm{HF}}$ with the local Kohn−Sham xc potential v_{xc}. Analyses of the linear response of the ground-state density calculated either with HF or with DFT to an external time-dependent perturbation lead to the TDHF or TDDFT schemes, respectively, as is indicated by the vertical arrows in Figure 1.

In analogy to the ground-state methods, TDHF and TDDFT are similarly related since the TDHF equations can be converted into the TDDFT equations by simply replacing the response of the HF exchange potential, $\partial v_{\mathrm{x}}^{\mathrm{HF}}/\partial\rho_1$, by the response of the xc potential from DFT, $\partial v_{\mathrm{xc}}/\partial\rho_1$. The Tamm−Dancoff approximation, that is, the neglect of the **B** matrix in the TDHF or TDDFT equations, leads in the TDHF case to CIS, while in the TDDFT case one obtains the TDDFT/TDA equations. Of course, CIS and TDDFT/TDA are equally related as TDHF and TDDFT are. However, in the case of CIS there exists a derivation route other than the Tamm−Dancoff approximation to TDHF, namely, via a CI formalism, that is, direct projection of the molecular Hamiltonian onto the "singly excited" Slater determinants. This is only possible because the projection of the Coulomb operator $\sum 1/(r_1 - r_2)$ contained in the molecular Hamiltonian yields terms equivalent to the response

of the Hartree−Fock exchange and Coulomb potential. Obviously, this is not the case for TDDFT/TDA, since the response of the xc potential contains the second derivative of the approximate local xc functional. Projection of the KS determinant would result in equations analogous to the CIS equation but the matrix elements evaluated for the KS orbitals.

3.4. Properties and Limitations

In section 3.2, it was presented how the linear response formulation of time-dependent density functional theory allows for the calculation of excitation energies and transition vectors in the DFT framework. At present, TDDFT represents one of the most prominent approaches for this task, especially when excited states of medium-sized or large molecular systems are under investigation.

Since the exact local xc potential, which is the key ingredient in DFT-based methods, is not known, an approximate xc functional has to be chosen in any practical calculation. Many different flavors of xc functionals are available today, for example, local functionals such as Slater−Vosko−Wilk−Nussair (SVWN),[56,81] gradient-corrected ones (GGAs) such as Becke−Lee−Yang−Parr (BLYP),[82,83] Perdew−Burke−Enzerhof (PBE),[84,85] or Becke−Perdew 1986 (BP86),[82,86] and hybrid functionals such as Becke3−Lee−Yang−Parr (B3LYP).[80] Moreover, the development of improved xc functionals is still a very active field of research. At present, the functionals B3LYP and PBE are the most widely used xc functionals in standard ground-state DFT applications, and although all these functionals have been developed with respect to the electronic ground state, they are also employed in TDDFT calculations, which is a consequence of the ALDA approximation (section 3.1.3). In many cases, results obtained with TDDFT are quite sensitive to the choice of the xc functionals, in particular, when local or GGA functionals are compared with hybrid functionals (see, for instance, refs 87 and 88). This aspect is also discussed in section 5.1. Therefore, the reliability of TDDFT calculations should always be checked by comparison with either wave-function-based benchmark calculations or experimental data, as well as by the sensitivity of the results to the choices of xc functional.

Although approximate xc functionals are employed in TDDFT, it has been proven to yield accurate results for valence-excited states the excitation energies of which lie well below the ionization potential. For such states, the typical error of TDDFT lies within the range of 0.1−0.5 eV, which is almost comparable with the error of high-level correlated approaches such as EOM-CCSD or CASPT2. However, to reach such high accuracy within the linear response formulation of TDDFT, one needs to include large sets of virtual orbitals. Still, in TDDFT, the accuracy is reached at very favorable computational cost making TDDFT applicable to fairly large molecules.

In general, the hybrid TDDFT scheme is solved analogously to the TDHF approach as it has been outlined in section 2.2.2. Again, the non-Hermitian eigenvalue problem (eq 88) can be converted into a Hermitian one, since the orbitals are usually real. It reads

$$(\mathbf{A}-\mathbf{B})^{1/2}(\mathbf{A}+\mathbf{B})(\mathbf{A}-\mathbf{B})^{1/2}\mathbf{Z}=\omega^2\mathbf{Z} \quad (97)$$

with

$$\mathbf{Z}=(\mathbf{A}-\mathbf{B})^{-1/2}(\mathbf{X}+\mathbf{Y}) \quad (98)$$

The solution of the hybrid TDDFT equations scales very similarly to the solution of the CIS and TDHF problems, which were already discussed in sections 2.1.2 and 2.2.2, respectively. However, hybrid TDDFT is slightly more expensive than TDHF since in addition to the response of the HF exchange, the response of the xc potential also needs to be evaluated. In common with ground-state DFT calculations, this is usually done numerically on an atom-centered three-dimensional quadrature grid.[89] With thresholding, this step can eventually scale linearly with the size of the molecule for sufficiently large systems, and thus eventually it becomes insignificant. The prefactor, however, is quite large, particularly for finer grids, and thus for medium-sized molecules, this step can dominate the computation.

When in addition only pure xc functionals are employed that do not include parts of HF exchange, the matrix $(\mathbf{A}-\mathbf{B})$ becomes diagonal (eq 89) and one can fully exploit this to avoid its multiplication with the trial vectors within the iterative Davidson scheme. In this case, the Tamm−Dancoff approximation does not imply a decrease in computational cost. On the contrary, as soon as hybrid functionals are used and $(\mathbf{A}-\mathbf{B})$ is thus not diagonal, the matrix multiplication must be performed and then TDDFT/TDA does save computation time by a factor of approximately two. Another algorithm to solve the TDDFT or TDHF response equations has been provided by Olsen et al.,[90] which exploits the specific paired structure of the non-Hermitian eigenvalue eq 90. This algorithm does not require the involved matrices to be explicitly available and thus allows for accurate calculations with high dimensions.

Additional computation time can be saved by a factor of 3−8 depending on the system of interest if the resolution-of-the-identity (RI) approximation[91] is used to evaluate the Coulomb-like terms of eq 96.[92,93] The RI approximation involves computational effort that scales with the cube of system size for Coulomb interactions (and the fourth power for HF exchange) for fixed basis set size. It is particularly valuable for medium and large atomic orbital basis sets because the cost for fixed molecule size grows only as $O(n^3)$, while conventional AO integral processing grows as $O(n^4)$. The additional error introduced in the excitation energies by the RI approximation is negligible since the larger errors in the total energies of the ground and excited states are subtracted out, making TDDFT applicable to very large molecular systems. On a modern computer, molecular systems with up to 3000 basis functions (approximately 200 first row atoms) can be treated by TDDFT in the standard implementation and systems with up to 4500 or so

basis functions (300 atoms) can be reached by TDDFT when the RI approximation is used.

The reason for the accuracy of TDDFT excitation energies is that the difference of the Kohn−Sham orbital energies, which are the leading term of the diagonal elements of the **A** matrix in eq 96, are usually excellent approximations for excitation energies.[94,95] This is because the virtual KS orbital energies are evaluated for the N-electron system and, thus, correspond more to the single-particle energy of an excited electron than to the energy of an additional electron as in Hartree−Fock theory, where the virtual orbital energies are evaluated for the $N + 1$ electron system. Consequently, orbital energy differences are a much better estimate for valence-excited states in KS-DFT than in HF theory. Although TDDFT performs usually very well for valence-excited states, it is now well-known that TDDFT has severe problems with the correct description of Rydberg states, valence states of molecules exhibiting extended π-systems,[96,97] doubly excited states,[98,99] and charge-transfer excited states.[100−103] For such states, the errors in the excitation energies can be as large as a few electronvolts, and the potential energy surfaces can exhibit incorrect curvature. The problems with Rydberg states and extended π-systems can be attributed to the wrong long-range behavior of current standard xc functionals, since they decay faster than $1/r$, where r is the electron−nucleus distance. For example, asymptotically corrected functionals such as van Leeuwen−Baerends 1994 (LB94)[104] or statistical averaging of orbital potentials (SAOP)[105] or local exact exchange potentials[106,107] yield substantially improved Rydberg state excitation energies.[108] States with substantial double excitation character cannot be treated within linear response theory in the usual ALDA approximation, since only singly excited states are contained in the linear response formalism.[98,99] They can however be recovered when the xc kernel is allowed to be frequency/energy dependent, since the xc kernel is in fact strongly frequency-dependent close to a double excitation.[98,99] In the case of excited charge-transfer (CT) states, which are the topic of section 3.5, the excitation energies are much too low and the potential energy curves do not exhibit the correct $1/R$ asymptote when R corresponds to a distance coordinate between the positive and negative charges of the CT state.

Since TDDFT and TDHF are very closely related linear response theories, it is not surprising that TDDFT possesses all the properties of TDHF (section 2.2.2). The linear response equations can be derived variationally,[66] but due to the approximate nature of the employed xc functionals, comparison with the exact total energy is not possible. One can say, though, that TDDFT is variational within the "model chemistry"[109] defined by the approximate xc functional. In analogy to TDHF, TDDFT is size-consistent, and it can yield pure spin singlet and triplet states for closed-shell molecules. Furthermore, TDDFT obeys the Thomas−Reiche−Kuhn sum rule of the oscillator strengths.[42]

Since 2002, analytic first geometric derivatives of the excitation energies given by the hybrid expression of TDDFT (eqs 88 and 96) are available,[65,66,110] which allow for the efficient calculation of first-order properties of excited states, for instance, their equilibrium geometries and dipole moments. The equilibrium structures, dipole moments, and harmonic frequencies of excited states calculated with TDDFT are of generally high quality, which is comparable to that of ground-state KS-DFT calculations.[66] So far, the analytic gradients have been implemented in CADPAC and TURBOMOLE.[48,49]

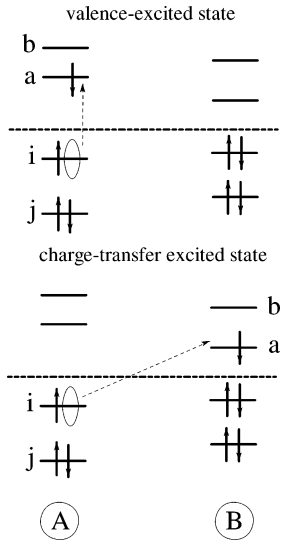

Figure 2. Schematic sketch of a typical valence-excited state, in which the transition occurs on one of the individual molecules, that is, the orbitals i, j and a, b are located on the same molecule in contrast to a charge-transfer excited state in which an electron is transferred from orbital i on molecule A to orbital a on molecule B. When the molecules A and B are spatially separated from each other the orbitals i and j do not overlap with a and b.

3.5. Charge-Transfer Excited States in TDDFT

As already mentioned in section 3.4, TDDFT yields substantial errors for charge-transfer excited states.[87,100,101,103,111] The excitation energies for such states are usually drastically underestimated, and moreover, the potential energy curves of CT states do not exhibit the correct $1/R$ dependence along a charge-separation coordinate R,[101,102,112] for in reality the positive and negative charges in a CT state electrostatically attract each other and, thus, separation of these charges must result in an attractive $1/R$ dependence. The wrong shape of the potential energy curves excludes the CT states from the reliable calculation of all molecular properties that involve their geometric derivative employing TDDFT or TDDFT/TDA.

These failures of TDDFT in the calculation of CT excited states can be understood by analysis of the basic eqs 88 and 96 for the case of charge-transfer excited states. In contrast to a valence-excited state, in a long-range, say for example, an intermolecular charge-transfer state, an electron is transferred from an occupied orbital i of molecule A to a virtual orbital a of another molecule B (Figure 2). For simplicity, let us assume that the overlap between orbitals on molecule A and orbitals on molecule B is zero.

Consequently, for such a state, all terms of eq 96 containing products of occupied and virtual orbitals vanish. This comprises the second and fourth term of the definition of the **A** matrix (eq 96) being the response of the Coulomb potential and the xc potential of the KS operator, respectively. Only the first term, which is the difference of the one-particle energies of the donor orbital i on A and the acceptor orbital a on B, and the third term originating from the nonlocal HF exchange part of the Kohn−Sham operator contribute to the **A** matrix of eq 86. This term contributes to the matrix elements of **A**, since orbitals i and j are both on A and the orbitals a and b are on B. In fact, this term is a Coulomb-like term, since the created holes (orbitals i and j corresponding to the positive charge in the CT state) interact with the electrons (orbitals a and b reflecting the negative charge), which relates to the electrostatic attraction within the CT state. Consequently, this term is essential for the correct $1/R$ dependence of the potential energy curves of CT states along the intermolecular separation coordinate. The same arguments are valid for the elements of the matrix **B** (eq 96), and all terms are zero, that is, this matrix does not contribute to CT states at all. For CT states, eq 96 reduces to the following simple expressions

$$A_{ia\sigma,jb\tau} = \delta_{\sigma\tau}\delta_{ij}\delta_{ab}(\epsilon_{a\sigma} - \epsilon_{i\tau}) - \delta_{\sigma\tau}c_{\mathrm{HF}}(i_\sigma j_\sigma|a_\tau b_\tau) \quad (99)$$

$$B_{ia\sigma,jb\tau} = 0 \quad (100)$$

It is now obvious from the definition of the **A** matrix in eq 100 that the excitation energy of a CT state in TDDFT is simply given by the difference of the orbital energies of the electron-accepting and electron-donating molecular orbitals, ϵ_a and ϵ_i, respectively, when a pure local xc functional (for instance, SVWN, BLYP,[82] or LB94) is employed, that is, $c_{\mathrm{HF}} = 0$. Within HF theory this is already a rough estimate for the energy of the CT state at large distances, since Koopman's theorem states that $-\epsilon_i$ and $-\epsilon_a$ correspond to the ionization potential of molecule A and to the electron affinity of molecule B, respectively. This is because the occupied orbitals are calculated for the N-electron system, while the virtual orbitals are formally evaluated for the $(N + 1)$-electron system. This is not the case in density functional theory following the Kohn−Sham formalism (DFT), since the same potential is used to calculate the occupied and virtual orbitals. As a consequence, while the HOMO still corresponds to the IP, the LUMO is generally more strongly bound in DFT than in HF theory and cannot be related to the EA. Since the negative of the LUMO energy is therefore much larger than the true EA, the orbital energy difference corresponding to a CT state is usually a drastic underestimation of its correct excitation energy. Furthermore, since the excitation energy of a CT state is simply given by the constant difference of the corresponding orbital energies, the potential energy curves of CT states do not exhibit the correct $1/R$ shape along a distance coordinate but are constant. As already mentioned, the electrostatic attraction between the positive charge (the holes i, j on A) and the negative charge (the electrons a, b on B) is contained in the second term of eq 100, which corresponds to the linear response of HF exchange. Therefore, the correct $1/R$ long-range behavior of the potential energy surfaces can in principle be recovered by inclusion of nonlocal HF exchange in the xc potential, which will improve the asymptotic behavior according to the factor c_{HF} of the exchange functional (eq 100). This explains the observed asymptotic behavior of potential energy curves of CT states of a tetrafluoroethylene−ethylene complex calculated with the SVWN, LB94, B3LYP, and "half-and-half" functional compared to configuration interaction singles (CIS) (Figure 3).[101]

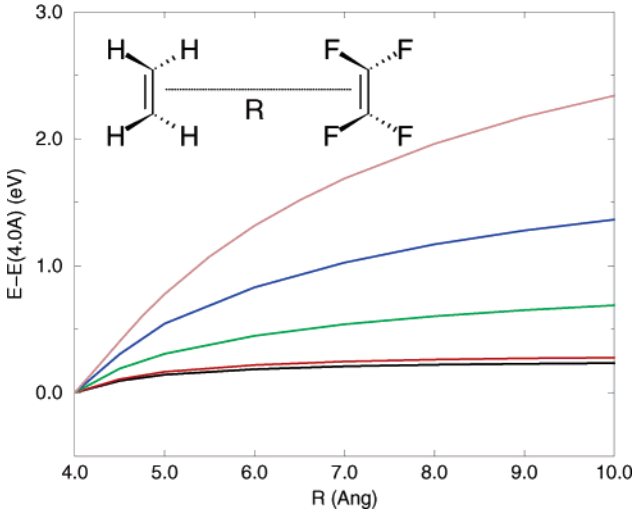

Figure 3. Comparison of the long-range behavior of the lowest CT excited state of an ethylene−tetrafluoroethylene dimer along the intermolecular separation coordinate computed with TDDFT employing the SVWN (black), LB94 (red), B3LYP (green), and "half-and-half" (blue) functionals with the curve obtained at the CIS (brown) level. The excitation energy of the lowest CT state at 4 Å is set to zero.

The $1/R$ failure of TDDFT employing pure standard xc functionals has in fact been understood as an electron-transfer self-interaction error. To clarify this, let us first inspect the case of TDHF ($c_{\mathrm{HF}} = 1$ in eq 90). The excitation energy of a long-range CT state, where an electron is excited from orbital i on molecule A into orbital a on molecule B, is dominated by the orbital energy difference $\epsilon_a - \epsilon_i$. In general, ϵ_a contains the Coulomb repulsion of orbital a with *all* occupied orbitals of the ground state including the orbital i, which is no longer occupied in the CT state. In other words, the electrostatic repulsion between orbitals a and i, the integral $(aa|ii)$, is contained in the orbital energy difference although orbital i is empty in the CT state. That means that the transferred electron in orbital a experiences the electrostatic repulsion with itself still being in orbital i, that is, it experiences molecule A as neutral. This electron-transfer self-interaction effect is canceled in TDHF by the response of the HF exchange term, the second term of the **A** matrix (eq 100), being $(ii|aa)$, which gives rise to the particle−hole attraction. In pure TDDFT employing approximate xc functionals, HF exchange is not present and the electron-transfer self-interaction effect is not exactly canceled leading to an incorrect long-range behavior of their potential

energy curves.

It is also worthwhile to note another peculiarity of CT states, namely, that the **B** matrix (eq 100) vanishes for a long-range CT state in the TDDFT, as well as TDHF, case. Since the neglect of the **B** matrix is equivalent to applying the Tamm−Dancoff approximation, TDHF and CIS, as well as TDDFT and TDDFT/TDA, yield identical results for the excitation energies of long-range CT states, which is the difference of the corresponding orbital energies. This fact can be exploited in TDDFT as a first diagnostic for whether one deals with a problematic CT state.

However, if the exact local Kohn−Sham xc potential would be used, which unfortunately is not known, the correct $1/R$ long-range behavior would be found. This is due to the derivative discontinuities of the exact exchange−correlation energy with respect to particle number.[112,113] In the case of an electron transfer from orbital i on molecule A to orbital a on molecule B, the xc potential jumps discontinuously by the constant $IP_A - EA_B$, leading to a singularity in the derivative of the xc potential with respect to the density, that is, the xc kernel f_{xc} used in the TDDFT calculation (eq 96). This singularity then compensates the vanishing overlap between the orbitals i and a when the molecules A and B are being separated, and thus, the fourth term of eq 96 does in fact contribute to a CT state when the exact xc potential would be employed, and the correct $1/R$ asymptote along the separation coordinate would then be obtained for a CT state. Furthermore, this clearly explains why standard approximate xc functionals in TDDFT fail in describing long-range CT states correctly since they do not contain the derivative discontinuities.

At present, several different pathways are starting to emerge to address this substantial failure of TDDFT for CT states and to correct for it. The most obvious way is to improve the xc functional by including exact exchange in the unperturbed Hamiltonian, either in the form of nonlocal Hartree−Fock exchange or of the exact local Kohn−Sham exchange potential. The latter are known as local Hartree−Fock (LHF) or also optimized effective potentials (OEPs), which have recently been introduced by Görling[106] and Ivanov et al.[107] These potentials may be able to yield the correct asymptotic $1/R$ dependence of excited CT states, since they possess singularities as soon as the overlap between the electron-donating and electron-accepting orbitals i and a, respectively, approaches zero. This, however, remains to be explored in detail, and it seems numerically difficult to compensate the vanishing overlap with the divergence of the xc kernel f_{xc} such that the fourth term of the **A** matrix (eq 96) cancels the electron-transfer self-interaction error correctly and recovers the correct $1/R$ asymptote. Also, satisfactory matching correlation functionals remain to be developed.

Inclusion of nonlocal Hartree−Fock exchange has been realized in a few schemes so far.[114−116] In all these schemes, the Coulomb operator of the Hamiltonian is split into two parts, a short-range and a long-range part, as, for example, in ref 114,

$$\frac{1}{r_{12}} = \frac{1 - \mathrm{erf}(\mu r_{12})}{r_{12}} + \frac{\mathrm{erf}(\mu r_{12})}{r_{12}} \qquad (101)$$

where $r_{12} = |r_1 - r_2|$. The first term of the right-hand side (rhs) corresponds to the short-range part and is evaluated using the xc potential from DFT, while the second term, the long-range part, is calculated with exact Hartree−Fock exchange. This idea is fairly old and had originally been suggested by Stoll and Savin already in 1985.[117−120] The scheme (eq 101) has been applied in combination with various xc functionals yielding, for instance, LC−BLYP, which indeed corrects the failures of TDDFT for CT excited states.[114] A major drawback of this approach, however, is that the standard xc functionals require a refitting procedure. Similar in spirit is the approach of Baer and Neuhauser, who also include long-range Hartree−Fock exchange but who employ a different partition function for the Coulomb operator.[116] An extension of this approach has been presented by Yanai et al., who combine B3LYP[80] at short range with an increasing amount of exact HF exchange at long range resulting in a functional called CAM-B3LYP,[115] which gives excellent CT excitation energies in comparison with benchmark calculations. But since they use at long range at most 60% HF exchange, the long-range asymptotic behavior of the CT states is not fully corrected.[115] A slightly different route is taken by Gritsenko and Baerends who suggest a new long-range corrected xc kernel that shifts the orbital energy of the acceptor orbital to a value related to the electron affinity. The wrong asymptotic behavior of the CT states is corrected by a distance-dependent Coulomb term correcting for electron-transfer self-interaction.[95]

A completely different ansatz to the solution of the CT problem may be represented by time-dependent current density functional theory (TDCDFT), which has recently been implemented in the Amsterdam density functional (ADF) package.[121,122] We have previously seen that a correct description of charge-transfer excited states requires the nonlocal HF exchange potential, and current functionals are nonlocal. However, at present no test calculation has yet been performed to show whether TDCDFT would in principle yield correct CT excited states. Also, due to its high computational cost the question remains whether this method will be applicable to large molecules soon.

4. Analysis of Electronic Transitions

When a molecule is excited from the electronic ground state to an energetically higher lying excited state, the electronic many-body wave function changes. To gain insight in the nature of the corresponding electronic transition, this change in the wave function needs to be analyzed. In principle, this is possible by direct analysis of the excited state wave function or its electron density. For this objective, the techniques developed for the analysis of the wave function or electron density of the ground state are simply applied to the excited state of interest. However, here we want to focus on approaches that are dedicated

to addressing differences in the ground state and excited state directly, avoiding tedious analysis of the excited-state wave function. These approaches comprise inspection of the molecular orbitals involved in the transition (section 4.1), the analysis of the transition density (section 4.2) or the difference density (section 4.3), and the so-called attachment/detachment density plots (section 4.4). The advantages and disadvantages of these analysis tools will be illuminated in the following subsections.

4.1. Molecular Orbitals

Usually, the electronic ground state of a molecular system can be represented by a single Slater determinant composed of single-electron wave functions describing the movement of the individual electrons in the molecule. These single-electron wave functions are the familiar molecular orbitals (MOs) well-known to chemists and often used to understand molecular processes. It is thus natural to analyze the changes in the many-body wave function, that is, the Slater determinant, in terms of the MOs that constitute it. As we have already seen in section 2.1, eq 7, an ansatz for an excited state wave function can be easily constructed by exchange of an occupied MO with a virtual one in the ground-state Slater determinant. Usually, an excited state is a linear combination of several such "excited" determinants, and the expansion coefficients are obtained by the corresponding calculation, in case of eq 7 by a CIS calculation. However, sometimes only one or two excited determinants contribute significantly to the excited-state wave function (i.e., $c_{ia} = 0.8-1.0$), and in such cases, it is easily possible to analyze the nature of the corresponding transition in terms of the occupied and virtual MOs that have been interchanged in the excited state determinants compared to the ground state. Such a case is, for instance, the charge-transfer excited state of the zincbacteriochlorin−bacteriochlorin complex investigated in section 5.2. The wave function of this excited state is composed of essentially one Slater determinant in which the highest occupied MO (HOMO) of the ground state is replaced with the lowest unoccupied MO (LUMO), since it has an expansion coefficient of 0.99 at the theoretical levels of TDDFT as well as CIS. Hence, the excited state corresponds to a single-electron transition from the HOMO to the LUMO (see also Figure 9 in section 5.2).

Although the analysis of an electronic transition via MOs is computationally easy and thus convenient and straightforward for states with only one or two significantly contributing Slater determinants, it can become very tedious for states that are represented by several determinants with expansion coefficients of similar size. Examples for this scenario are the wave functions of the repulsive excited states of CO-ligated heme, the investigation of which is described in section 5.1. These states are represented by a linear combination of four "singly excited" determinants with coefficients between 0.3 and 0.7, thus making it almost impossible to obtain a clear picture of the nature of these electronic transitions based on MOs.

4.2. Transition Density

Another possibility to obtain information about an electronic transition is to analyze the one-electron transition density. The transition density, $T(r)$, couples the electronic ground state with the excited state of interest and is in general given as

$$T(r) = N\int |\Psi_{ex}(r_1,r_2,...r_n)\rangle\langle\Psi_0(r_1,r_2,...r_n)|\, dr_2...dr_n \quad (102)$$

If the electronic ground state is given as a single Slater determinant and the electronically excited state of interest as a linear combination of determinants, then $T(r)$ is given as a linear combination of single-determinant transition densities weighted by their expansion coefficients

$$T(r) = \sum_{ia} c_{ia}\int |\Phi_{ia}(r_1,r_2,...r_n)\rangle\langle\Phi_0(r_1,r_2,...r_n)|\, dr_2...dr_n \quad (103)$$

In principle, one can analyze the transition density directly to obtain valuable information about the symmetry of the transition and about the way in which a one-electron operator couples two different states. It is however useful to analyze the transition density matrix, which is given in the molecular orbital basis as

$$\mathbf{T}_{ia} = \langle\phi_i|\hat{T}(r)|\phi_a\rangle \quad (104)$$

via so-called "natural transition orbitals" (NTOs) analogous to the well-known natural orbitals obtained by diagonalization of the ground-state single-electron density.[123] Since the transition density matrix is a rectangular $n_{occ} \times n_{virt}$ matrix, it cannot simply be diagonalized. Instead, the "corresponding orbital transformation" by Amos and Hall[124] can be applied, which is based on a singular value decomposition of the transition density matrix

$$\mathbf{T} = \mathbf{USV}^\dagger \quad (105)$$

where $\mathbf{U}$ and $\mathbf{V}$ are $n_{occ} \times n_{occ}$ and $n_{virt} \times n_{virt}$ unitary matrices, respectively, and $\mathbf{S}$ is a singular matrix containing the singular values of $\mathbf{T}$. In general, one can write

$$\begin{aligned}\mathbf{TT}^\dagger &= \mathbf{USV}^\dagger\mathbf{VS}^\dagger\mathbf{U}^\dagger \\ &= \mathbf{USS}^\dagger\mathbf{U}^\dagger \\ &= \mathbf{US}^2\mathbf{U}^\dagger\end{aligned} \quad (106)$$

from which follows that

$$\mathbf{U}^\dagger\mathbf{TT}^\dagger\mathbf{U} = \mathbf{S}^2 \quad (107)$$

that is, the unitary transformation $\mathbf{U}$ diagonalizes the matrix $\mathbf{TT}^\dagger$ and consequently contains its eigenvectors as columns. The singular values of $\mathbf{S}$ are given as the square root of the eigenvalues of $\mathbf{TT}^\dagger$. Therefore, one can determine the unitary transfor-

mation matrix **U** and the singular matrix **S** by solving the eigenvalue equation

$$\mathbf{T}\mathbf{T}^{\dagger}\vec{u}_i = \lambda_i\vec{u}_i \qquad i = 1, 2, ..., n_{\mathrm{occ}} \qquad (108)$$

Following an argument for the matrix $\mathbf{T}^{\dagger}\mathbf{T}$ analogous to eq 106 one finds that the unitary matrix **V** can be determined by solving a corresponding eigenvalue equation

$$\mathbf{T}^{\dagger}\mathbf{T}\vec{v}_i = \lambda_i\vec{v}_i \qquad i = 1, 2, ..., n_{\mathrm{virt}} \qquad (109)$$

Although the matrices $\mathbf{T}\mathbf{T}^{\dagger}$ and $\mathbf{T}^{\dagger}\mathbf{T}$ have different dimensions, namely, $n_{\mathrm{occ}} \times n_{\mathrm{occ}}$ and $n_{\mathrm{virt}} \times n_{\mathrm{virt}}$, respectively, their first n_{occ} eigenvalues are identical, and the eigenvalues $\lambda_{n_{\mathrm{occ}}}...\lambda_{n_{\mathrm{virt}}}$ of the larger matrix $\mathbf{T}^{\dagger}\mathbf{T}$ are zero in the case of CIS or TDA

$$1 \geq \lambda_i = \lambda_i' \geq 0 \qquad i = 1, 2, ..., n_{\mathrm{occ}}$$

$$\sum_i^{n_{\mathrm{occ}}} \lambda_i = 1$$

$$\lambda_i = 0 \quad i = (n_{\mathrm{occ}} + 1), ..., n_{\mathrm{virt}} \qquad (110)$$

These additional zero eigenvalues arise from mapping the original transition density matrix onto the larger matrix $\mathbf{T}^{\dagger}\mathbf{T}$, and hence the additional eigenvectors and eigenvalues must belong to the kernel of the map. In the case of TDHF or TDDFT, the sum of the eigenvalues will not be identical to one but will deviate from that to the extent that the de-excitations are significant. Especially in TDDFT, these contributions are usually small.

The occupied and virtual "natural transition orbitals", ϕ_i^{nto} and ϕ_a^{nto}, respectively, are defined as

$$\phi_i^{\mathrm{nto}} = \phi_i\mathbf{U} \qquad i = 1, 2, ..., n_{\mathrm{occ}} \qquad (111)$$

$$\phi_a^{\mathrm{nto}} = \phi_a\mathbf{V} \qquad a = 1, 2, ..., n_{\mathrm{occ}} \qquad (112)$$

where in eq 112 the index a ends at n_{occ} and not n_{virt}, since $n_{\mathrm{virt}} - n_{\mathrm{occ}}$ virtual orbitals are mapped onto the null vector. Following this procedure, a one-to-one mapping between occupied and virtual orbitals is established, because one occupied and one virtual NTO correspond to each eigenvalue λ_i.

In summary, the originally $n_{\mathrm{occ}} \times n_{\mathrm{virt}}$ dimensional transition density matrix has been reduced to a $n_{\mathrm{occ}} \times n_{\mathrm{occ}}$ dimensional matrix in the basis of so-called "natural transition orbitals", which correspond to n_{occ} particle−hole amplitudes. With each hole in the occupied space, one single corresponding particle in the virtual space can be associated by means of the associated eigenvalue λ. The importance of a particular particle−hole excitation to an electronic excitation is reflected by the value of the corresponding eigenvalue. Usually, electronic transitions can be expressed by one single particle−hole pair in the NTO basis with an associated eigenvalue of essentially one, even such transitions that are highly mixed in the canonical molecular orbital basis. Plotting the corresponding NTOs gives detailed insight into the nature of the electronic transition.

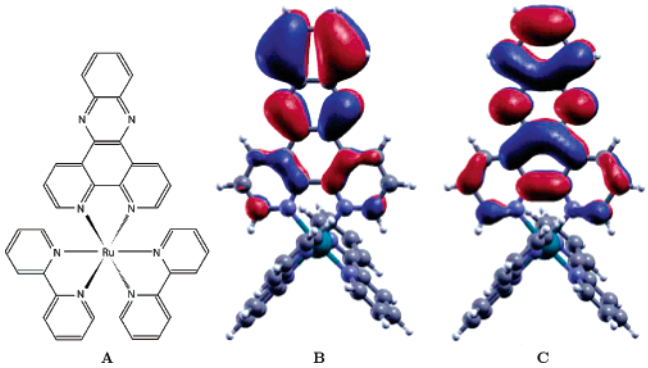

Figure 4. Molecular structure (A) and NTOs of the hole (B) and particle (C) densities of the lowest $^3\pi-\pi^*$ transition of $[Ru(bpy)_2dppz]^{2+}$.[125]

An example for the successful application of NTOs is the analysis of the nature of the energetically lowest excited states of the ruthenium complex $[Ru(bpy)_2dppz]^{2+}$ (bpy = 2,2′-bipyridine; dppz = dipyrido[3,2-*a*:2′,3′-*c*]phenazine, which serves as very sensitive luminescent reporter of DNA in aqueous solution.[125] In Figure 4, the molecular structure of the complex and the NTOs of the hole and particle of the lowest $^3\pi-\pi^*$ transition are given. In this case, an analysis of the involved molecular orbitals is very tedious since the transition is represented by a linear combination of several singly substituted determinants, while on the contrary, the natural transtion orbitals capture 90% of the character of the transition. More examples for the application of analyses via NTOs can be found in refs 123, 125, and 126.

4.3. Difference Density

A complementary approach to the analysis of the transition density matrix **T** is the investigation of the difference density matrix **Δ**, which is simply given as the difference between the single electron density matrices of the excited state $\mathbf{P}_{\mathrm{ex}}$ and the electronic ground state $\mathbf{P}_0$

$$\mathbf{\Delta} = \mathbf{P}_{\mathrm{ex}} - \mathbf{P}_0 \qquad (113)$$

Today, the analysis of an electronic transition by means of the difference density is frequently performed (see, for example, refs 127−130), and in principle, valence and Rydberg excited state can be easily distinguished. Also the nature of the transition (n−π^* or charge-transfer) is often readily apparent for simple molecular systems. However, the difference density is a complicated function with often intricate nodal surfaces, which makes its plotting and analysis often very tedious especially for larger molecules. This is mostly because both the ground-state electron density that is removed upon excitation and the "new" electron density of the excited state are shown with different signs together in one picture. It is also somewhat awkward that a density acquires a negative sign since it is originally defined as the square of the wave function.

4.4. Attachment/Detachment Density Plots

The physically most appealing and conceptually easiest way to analyze the nature of a complicated electronic transition is via so-called attachment/detachment density plots.[32,131] The basis of this analysis is the diagonalization of the difference density matrix $\mathbf{\Delta}$ given by eq 113 in section 4.3 via

$$\mathbf{U}^{\dagger}\mathbf{\Delta}\mathbf{U} = \delta \tag{114}$$

where $\mathbf{U}$ is a unitary transformation matrix containing the eigenvectors of the difference density matrix, which again could be considered as "natural orbitals of the electronic transition" but which are generally different from those in section 4.2. δ is the diagonal matrix containing the eigenvalues δ_p of $\mathbf{\Delta}$, which are interpreted as occupation numbers of the eigenvectors. The difference density matrix is a square $N \times N$ dimensional matrix, where N is $(n_{\mathrm{occ}} + n_{\mathrm{virt}})$. In electronic transitions that do not involve ionization or electron attachment, the sum of all occupation numbers must be zero; otherwise it corresponds to the net electron gain or loss of electrons n during the transition, that is,

$$Tr(\mathbf{\Delta}) = \sum_{p=1}^{N} \delta_p = n \tag{115}$$

In a next step, the diagonal difference density matrix δ is split into two matrices $\mathbf{A}$ and $\mathbf{D}$. The matrix $\mathbf{D}$, the so-called detachment density, is defined as the sum of all eigenvectors of $\mathbf{\Delta}$ that possess negative eigenvalues, weighted by their absolute value of their occupations. Consequently, if $\mathbf{d}$ is a diagonal matrix with elements

$$d_p = -\min(\delta_p, 0) \tag{116}$$

then

$$\mathbf{D} = \mathbf{U}\mathbf{d}\mathbf{U}^{\dagger} \tag{117}$$

The detachment density matrix $\mathbf{D}$ is a positive semidefinite $N \times N$ matrix, since the sign of the negative eigenvalues is changed, and thus, it has positive entries everywhere, where $\mathbf{\Delta}$ has negative ones. All other values of $\mathbf{\Delta}$ are set to zero. This density corresponds to the electron density of the ground state that is removed upon electron excitation and can thus be seen as a hole density, although not in general corresponding to removal of an integral number of electrons.

The attachment density matrix $\mathbf{A}$ is similarly defined as the sum of all natural orbitals of the difference density matrix with positive occupation numbers, weighted by the absolute value of their occupation. Consequently, if $\mathbf{a}$ is a $N \times N$ diagonal matrix with elements

$$a_p = \max(\delta_p, 0) \tag{118}$$

then

$$\mathbf{A} = \mathbf{U}\mathbf{a}\mathbf{U}^{\dagger} \tag{119}$$

This density matrix $\mathbf{A}$ corresponds to the particle levels occupied in the electronic transition. The difference between the two new matrices $\mathbf{A}$ and $\mathbf{D}$ corresponds to the original difference density matrix $\mathbf{\Delta}$:

$$\mathbf{\Delta} = \mathbf{A} - \mathbf{D} \tag{120}$$

In other words, the detachment density is that part of the single-electron ground-state density that is removed and rearranged as attachment density. Together these densities characterize an electronic transition as $\mathbf{D} \rightarrow \mathbf{A}$, which permits the visualization and analysis of electronic transitions more or less as if they correspond to just single-orbital replacements, regardless of the extent of configuration mixing that occurs in the excited-state wave function and regardless of how inappropriate the molecular orbitals are for the description of the transition. The analysis via attachment/detachment density plots can be applied to any excited-state calculation that yields a one-particle difference density.

An application of attachment/detachment density plots is given in section 5.1, where the excited states of CO-ligated heme are analyzed (Figure 7). These states are characterized by strong configuration mixing of four excited Slater determinants, which makes an analysis in the molecular orbital basis impossible. By means of attachment/detachment plots, the nature of the repulsive states could be easily analyzed and understood in terms of an Fe−CO back-bonding to anti-back-bonding transition. Further applications of attachment/detachment plots can be found, for example, in refs 132−135.

5. Illustrative Examples

In this section, illustrative and educative examples for applications of CIS, TDHF, and TDDFT to large molecular systems will be presented. First, an investigation of the ultrafast photodissociation process of CO-ligated heme employing TDDFT is described, which is a well suited model study, since it demonstrates the necessity to perform a detailed investigation of the functional performance and it highlights the usefulness of attachment/detachment density plots to analyze complicated electronic transitions. Then, we will show TDDFT results for a zincbacteriochlorin−bacteriochlorin complex, where we are interested in the spectral properties of the complex in comparison to the individual molecules. Here, severe problems with charge-transfer excited states are encountered using TDDFT alone, and a practical hybrid approach combining the benefits of TDDFT and CIS must be applied to obtain physically reasonable results. During the whole section, emphasis is put on the theoretical approach and the choice of method rather than on the chemically and physically interesting results of the investigations, which can be found in the original publications.

5.1. The Initial Steps of the Ultrafast Photodissociation of CO-Ligated Heme

CO-ligated iron porphyrin (heme) is known to undergo ultrafast dissociation of the CO ligand

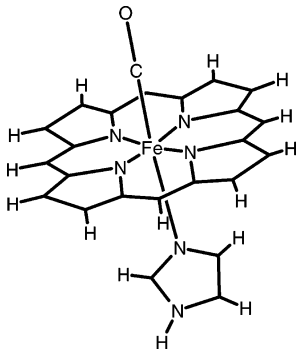

Figure 5. Model complex used for the theoretical investigation of CO-ligated heme.

within 50 fs upon excitation of the system in the energetically lowest lying *Q*-states of the porphyrin ring.[136] In a recent theoretical investigation employing TDDFT, the electronically excited states of CO-ligated heme were studied with the objective to identify and characterize the electronic states that are involved in the ultrafast photodissociation process.[88,137] Within the calculation, a model complex was used that reflects the structural characteristics of the heme group in the intact proteins hemoglobin and myoglobin (Figure 5).

A crucial step in theoretical investigations employing TDDFT is the choice of an appropriate exchange−correlation (xc) functional and a reasonable basis set. Since one cannot expect that one approximate xc functional describes all excited states of a molecule equally well, it is important to test several xc functionals with respect to their performance for the system under investigation. In principle, calculated properties are compared with their experimental values, for example, geometrical parameters or experimentally determined excitation energies of optically allowed transitions. In the presented investigation of the CO-ligated heme group, the geometrical parameters optimized with ground-state DFT, as well as the values of the experimentally observable electronic transitions, the Q and B states, calculated with TDDFT, are compared with their experimental values. Three different xc functionals were tested: the local Slater−Vosko−Wilk−Nusair (SVWN) functional,[56,81] the gradient-corrected Becke−Lee−Yang−Parr (BLYP)[82] functional, and the hybrid Becke3−Lee−Yang−Parr (B3LYP)[80] functional. As first test, the geometries of the complex were optimized using standard ground-state DFT with the three xc functionals mentioned above and the LANL2DZ basis set, which makes use of the Los Alamos effective core potential for the inner electron shell of the iron atom and uses the 6-31G basis set on all other lighter atoms. The calculated values for four selected parameters (the Fe−CO bond, the bond between the iron and the porphyrin nitrogens (Fe−N_P), the bond between the iron and the imidazole nitrogen (Fe−N_{Im}), and the C−O bond of the CO ligand) are given in Table 1 and compared with their experimental values.[138,139] It can be seen that the calculated values depend only slightly on the quality of the xc functional, that is, they are essentially independent of the choice of the functional.

Table 1. Calculated Geometrical Parameters (Å) of the CO-Ligated Heme Model Complex in Comparison with Experimentally Determined Values for the Complete System

	BLYP	B3LYP	expt
Fe−CO	1.81	1.80	1.73−1.93
Fe−N_P	2.01	2.03	1.98−2.06
Fe−N_{Im}	1.98	2.04	2.06−2.20
C−O	1.21	1.16	1.07−1.12

Table 2. Excitation Energies (eV) of the Q and B States of the Model Complex Compared with the Experimentally Observed Values

	SVWN		BLYP		B3LYP		
	LANL2DZ	6-31G*	LANL2DZ	6-31G*	LANL2DZ	6-31G*	expt
Q_y	1.515	1.396	1.833	1.573	2.404	2.403	2.18
Q_x	1.537	1.418	1.843	1.593	2.418	2.413	2.30
B_x	3.009	2.909	3.049	2.927	3.347	3.314	2.96
B_y	3.020	2.927	3.056	2.943	3.359	3.325	3.16

As second test of the functional performance, the excited states of the model complex were calculated using TDDFT employing the functionals from above, and the obtained values were compared with the experimentally known values of the excitation energies of the allowed transitions, the Q and B states.[140] The Q and B states are known to be $\pi-\pi^*$ transitions and can thus be expected to be reasonably well described by TDDFT. For these test calculations, the standard 6-31G* basis set and the LANL2DZ basis set were employed. The results of the test calculations are summarized in Table 2.

In contrast to the geometrical parameters, which varied only slightly when different xc functionals were tested, the excitation energies are sensitive to the choice of the xc functional. While the local SVWN and the gradient-corrected BLYP functional strongly underestimate the excitation energies of the Q states, the B bands are in good agreement with the experimental values. The hybrid B3LYP functional, however, overestimates the excitation energies of both the Q states and the B states by about 0.2 eV. After a closer look at the basis set dependence, the results of the SVWN and BLYP calculations change strongly when going from the LANL2DZ basis set to the 6-31G* basis set. This is not the case for the calculations employing the B3LYP functional. Due to the consistent error of 0.2 eV for all tested states and the robustness of the B3LYP functional with respect to basis set change, the B3LYP functional has been chosen to be the one used throughout the whole investigation of the photodissociation process of CO-ligated heme. This investigation clearly illustrates the importance of a performance check of the xc functionals prior to the actual investigation. As one can see, it is not possible to pick one random functional and be guaranteed to obtain reliable results for excitation energies within the TDDFT framework.

To identify the relevant excited electronic states for the ultrafast photodissociation process of CO-ligated heme, the lowest excited singlet states of the system were calculated along the CO stretch coordinate employing TDDFT in combination with the B3LYP functional and the LANL2DZ basis set. The

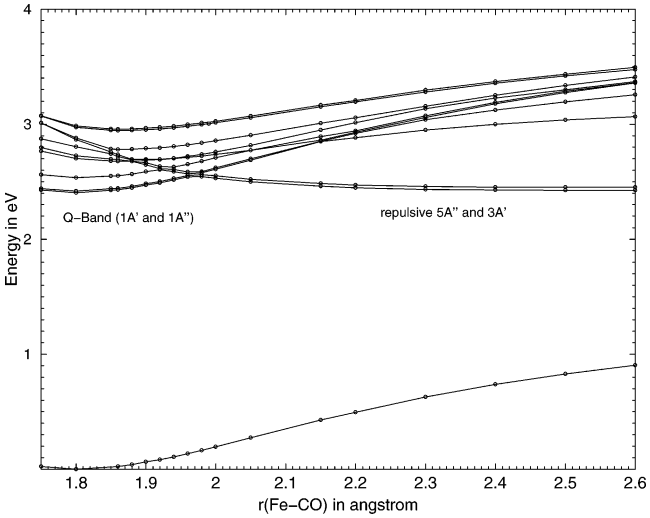

Figure 6. Calculated potential energy curves along the Fe−CO stretch coordinate for CO-ligated heme. The data have been obtained using TDDFT/B3LYP/LANL2DZ.

geometry of the system was not optimized along the dissociation pathway, since geometry relaxation effects can be expected to be small for this ultrafast process. The calculated potential energy curves are shown in Figure 6.

Upon photoexcitation of CO-ligated heme into the Q states (1A′ and 1A″ in Figure 6), the system decays nonradiatively into two quasi-degenerate repulsive states. These states are identified as 3A′ and 5A″ at the equilibrium geometry of CO-ligated heme. Along the dissociation coordinate, a small energy barrier of 0.15 eV must be crossed, but this is probably easily accomplished by vibrational excitation going along with the photoexcitation. Calculation of the vibrational frequencies of the electronic ground state with DFT/B3LYP/6-31G* corroborates this picture, since the period of the vibration associated with the Fe−CO stretch coordinate is calculated to be about 70 fs, which strongly correlates with the time scale of the photodissociation process of 50 fs.

Since the repulsive excited states involve linear combinations of several molecular orbitals and are, thus, difficult to analyze in terms of orbitals, the nature of the repulsive states has been analyzed using attachment/detachment density plots[32] (see also section 4.4) at the equilibrium geometry, as well as at an Fe−CO bond length of 2.5 Å. The calculated plots are displayed in Figure 7. Comparison of the detachment and attachment densities nicely explains the repulsive character of the 5A″ and 3A′ states at the equilibrium geometry (upper panel of Figure 7). While the detachment density, which is removed from the ground-state density, is clearly dominated by a bonding iron−carbon interaction, the attachment density, which is added to the ground-state density, has clearly antibonding character, which is seen as a node along the Fe−C bond. The bonding interaction between the iron atom and the CO ligand in the detachment density can be understood in chemical terms as back-bonding from an iron d-orbital into the π^* orbital of CO. The antibonding interaction in the attachment density corresponds to the antibonding combination of these orbitals (anti-back-bonding). Furthermore, it can be seen from the attachment/detachment density plots of the repulsive states at 2.5 Å Fe−CO bond distance (lower panel of Figure 7) that the character of this state changes along the Fe−CO stretch coordinate and that it gets more iron d-orbital character.

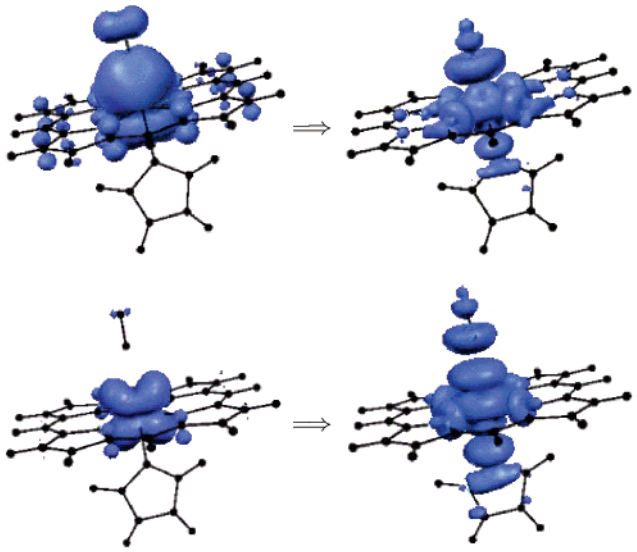

Figure 7. Attachment/detachment density plots of the repulsive states calculated at the equilibrium Fe−CO distance of 1.8 Å (top) and at an Fe−CO bond length of 2.5 Å (bottom) using TDDFT/B3LYP/LANL2DZ. The isosurfaces shown are calculated for a 90% density enclosure.

In summary, application of TDDFT to the ultrafast photodissociation of CO-ligated heme has led to a detailed understanding of the initial steps of this complicated process. Furthermore, the presented investigation can serve as a good example for a typical TDDFT study, since the excited electronic states under investigation are typical valence-excited states, which can be expected to be reasonably well described with TDDFT. A detailed study of the dependence of the results on different xc functionals has been performed, which is a crucial step in any theoretical investigation employing TDDFT. The usefulness of density-based analyses, here attachment/detachment density plots, has been demonstrated.

5.2. Charge-Transfer Excited States in Zincbacteriochlorin–Bacteriochlorin Complexes

Despite its failure for CT states as outlined in section 3.5, TDDFT has recently been applied to several molecular complexes in which photoinitiated electron transfer might occur and, thus, long-range CT excited states are relevant. In this spirit, phenylene-linked free-base porphyrin and zincporphyrin complexes, as well as their bacteriochlorin (BC) analogues, have been investigated employing TDDFT in combination with the BLYP functional,[141,142] and a plethora of spurious CT states was obtained in the visible range of the electronic spectra of these compounds. In contrast, in a similar study of linked zincporphyrin dimers in which the symmetry-adapted cluster configuration interaction (SAC-CI) method[27] has been employed, CT excited states were not found in the energy regime of the energetically lowest Q

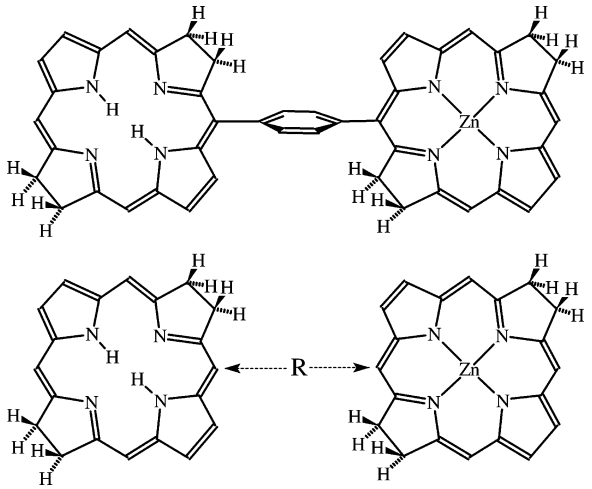

Figure 8. Molecular structure of the (1,4)-phenylene-linked zincbacteriochlorin−bacteriochlorin complex, as well as of the model complex used in some calculations. The distance coordinate R is here defined as the distance between the formerly linked carbon atoms.

states of zincporphyrins,[143] which is in accordance with experimental findings (see ref 144 and references herein). Typically, charge-transfer excited states are experimentally identified via polarity dependent solvatochromic shifts of their absorption band or by means of ultrafast transient absorption spectroscopy.[145−147] In this section, we are going to outline a recent reinvestigation of the excited states of a phenylene-linked zincbacteriochlorin−bacteriochlorin complex (Figure 8) employing TDDFT[102] for two reasons. On one hand, we want to demonstrate the substantial failure of TDDFT employing standard xc functionals for CT excited states, and on the other hand, the usefulness of the practical scheme to circumvent the problem introduced in here should be pointed out.

As a first step, the excited states of the monomers zincbacteriochlorin and bacteriochlorin have been calculated employing TDDFT with the BLYP[82] xc functional and the 6-31G* basis set at the separately optimized geometries. At this level of theory, ZnBC possesses weakly allowed singlet excited states at 2.07 and 2.44 eV, as well as strongly allowed transitions at 3.62 and 3.88 eV, which are interpreted as the well-known Q_x and Q_y, as well as B_y and B_x, states, respectively. The corresponding states of bacteriochlorin are found at energies of 2.10 (Q_x), 2.39 (Q_y), 3.67 (B_y), and 3.85 eV (B_x). Our calculated as well as experimental values for the excitation energies of the Q states are given in Table 3.

All values are in reasonable agreement with other calculations of the electronic absorption spectra of ZnBC and BC.[148−150] Using the same theoretical approach for the calculation of the 10 lowest singlet excited states of the full (1,4)-phenylene-linked ZnBC−BC complex (Figure 8), one obtains the values given in Table 3. As expected, the Q-states of the constituting monomers are found at almost exactly identical energies in the linked complex. They are slightly red-shifted by only 0.01−0.02 eV. In addition to the monomer states, further energetically low-lying states are found at 1.33, 1.46, 1.86, and 1.94 eV. The

Table 3. Comparison of the Energies of the Ten Lowest Singlet Excited States of the Full Phenylene-Linked ZnBC−BC Complex as Well as of the Model Complex without the Phenylene Bridge with the Individually Calculated and Experimentally Determined Excitation Energies of the Q States of the Monomers[a]

	ZnBC−BC complex			monomers	
state	full	model	transition	calcd	expt
1	1.33 (0.000)	1.32 (0.000)	ZnBC → BC CT		
2	1.46 (0.000)	1.47 (0.000)	BC → ZnBC CT		
3	1.86 (0.000)	1.90 (0.000)	BC → ZnBC CT		
4	1.94 (0.001)	1.96 (0.000)	ZnBC → BC CT		
5	2.05 (0.393)	2.07 (0.266)	$\pi-\pi^*$ ZnBC (Q_x)	2.07 (0.231)	1.65[b]
6	2.09 (0.131)	2.12 (0.170)	$\pi-\pi^*$ BC (Q_x)	2.10 (0.187)	1.6[c]
7	2.38 (0.059)	2.40 (0.038)	$\pi-\pi^*$ BC (Q_y)	2.39 (0.034)	2.3[c]
8	2.42 (0.019)	2.46 (0.018)	$\pi-\pi^*$ ZnBC (Q_y)	2.44 (0.026)	2.2[b]
9	2.43 (0.022)	2.42 (0.000)	ZnBC → BC CT		
10	2.58 (0.000)	2.66 (0.000)	BC → ZnBC CT		

[a] The oscillator strength of each transition is given in brackets behind the corresponding energy. All calculations have been performed at the level of TDDFT/BLYP/6-31G* and all energies are given in eV. [b] Experimental data for zinctetraphenylbacteriochlorin−pyridine were taken from ref 154. [c] Experimental data for bacteriopheophorbide were taken from ref 155.

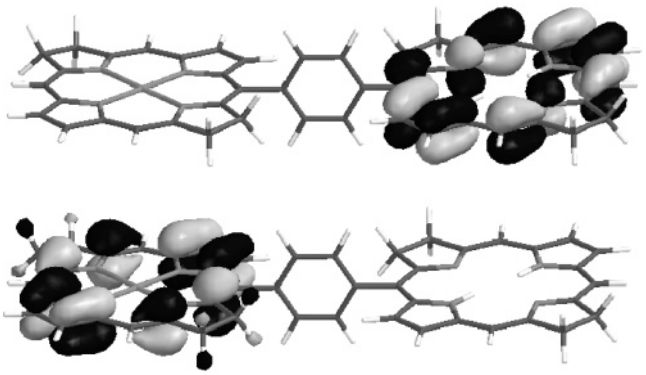

Figure 9. Highest occupied molecular orbital (HOMO, bottom) and lowest unoccupied molecular orbital (LUMO, top) of the ZnBC−BC complex. In the lowest excited CT state, an electron is transferred from the HOMO to the LUMO, and thus, this transition corresponds to an electron transfer from ZnBC to BC.

energetically lowest state at 1.33 eV is a pure one-electron transition from the highest occupied molecular orbital (HOMO) into the lowest unoccupied molecular orbital (LUMO), and analysis of these MOs (Figure 9) clearly shows that this state corresponds to an electron transfer from ZnBC to BC. In analogy, states 2 and 3 at 1.46 and 1.86 eV represent BC-to-ZnBC CT states, while state 4 at 1.94 eV is again a ZnBC-to-BC CT state. Of course, these states cannot be present if the monomers are calculated individually but are a characteristic of complex formation.

However, as pointed out in section 3.5, the calculated values of the CT states are given at too low energies, which can be easily confirmed by simple electrostatic considerations. Assuming that the separated charges in the CT states could be treated as point charges, the distance-dependent excitation energy of the energetically lowest ZnBC-to-BC CT state $\omega_{CT}(R)$ can simply be estimated via

$$\omega_{CT}(R) > IP_{ZnBC} + EA_{BC} - 1/R \qquad (121)$$

where IP_{ZnBC} is the ionization potential of the ZnBC monomer, EA_{BC} is the electron affinity of bacteriochlorin, and $1/R$ is the electrostatic attraction between them. Of course, R corresponds to the distance between the charges, which in our approximation is chosen to be the smallest distance between the carbon atoms of the different tetrapyrrol rings in the (1,4)-phenylene-linked ZnBC−BC complex, which has a value of 5.84 Å (see also Figure 8). At the level of DFT/BLYP/6-31G*, IP_{ZnBC} has a value of 5.57 eV and EA_{BC} is given as −0.42 eV yielding an excitation energy for the lowest ZnBC-to-BC CT state of about 2.69 eV at the equilibrium distance R of the linked complex. In this equation, the cation and anion are treated as point charges and the shortest possible distance R is assumed, which of course leads to an overestimation of the electrostatic attraction. As a consequence, the estimated excitation energy ω_{CT} is a true lower bound to the correct value. Comparison with the excitation energy calculated at the level of TDDFT/BLYP/6-31G*, which has a value of 1.33 eV, yields a minimum error of 1.36 eV for this CT state. This demonstrates the tendency of TDDFT to underestimate the excitation energies of CT states drastically. It is worthwhile to note that the excitation energies of the CT states computed with TDDFT correspond in fact exactly to the difference of the orbital energies involved in the excitations, as we have already discussed in section 3.5. For instance, the excitation energy of the lowest CT state (1.33 eV) is solely given by the difference of the HOMO (−3.70 eV) and LUMO (−2.37 eV) energies of the electronic ground state.

As the next step, the dependence of the excitation energies of the lowest CT states on the distance R between the separated charges will be investigated. This requires the introduction of a suitable model complex, in which the distance between the positive and negative charges of the CT state can be easily varied. For the (1,4)-phenylene-linked ZnBC−BC complex, this is easily accomplished by neglecting the phenylene bridge, and choosing the distance between the formerly connected carbon atoms as the distance coordinate R, which has a value of 5.84 Å in the linked complex and was used previously to estimate the minimum excitation energy, ω_{CT}, in eq 121. As can be seen in Table 3, the phenylene bridge has only minor influence on the 10 lowest excited states of the complex, which are slightly shifted by an average of 0.03 eV, while the largest shift of 0.08 eV occurred for state 10. As a consequence, the model complex can be used in further calculations without losing general validity of the obtained results.

To investigate the asymptotic behavior of the excited states and, in particular, of the excited CT states of the ZnBC−BC complex, the 10 lowest excited states of the model complex (Figure 8) have been calculated employing TDDFT with the BLYP functional and the 6-31G* basis set along the distance coordinate R. The obtained potential energy curves (PECs) are displayed in the upper part of Figure 10. As can be easily seen, the potential energy curves of the CT states are constant along the distance R between the monomers (the excitation

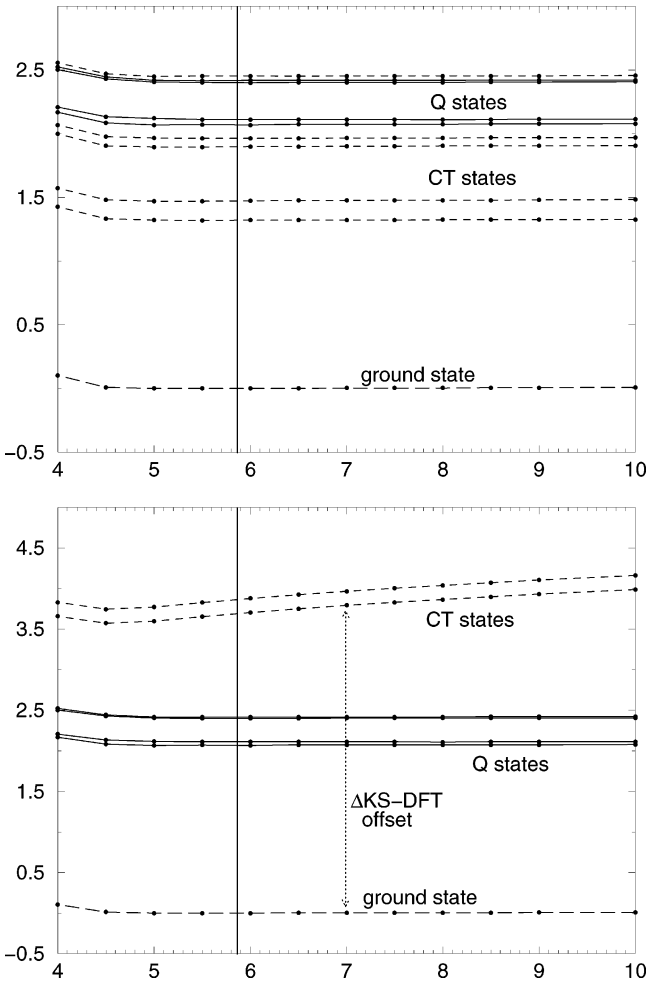

Figure 10. Potential energy curves of the lowest singlet excited states of the ZnBC−BC complex along the distance coordinate R calculated with TDDFT/BLYP/6-31G* (top) and with the hybrid TDDFT/CIS approach (bottom, see text for details). Short-dashed lines correspond to CT excited states, solid lines are the valence-excited Q states, and the long-dashed line represents the electronic ground state.

energies correspond to the orbital energy differences), and they do not show the correct $1/R$ dependence. This is due to the electron-transfer self-interaction, which is not canceled in the employed pure BLYP functional as we have outlined in section 3.5. In the lower part of Figure 10, potential energy curves are shown that are obtained with a hybrid approach of TDDFT and CIS that will be described in detail within the next paragraph.

In contrast to TDDFT methods, CIS and TDHF yield the correct $1/R$ behavior of the potential energy curves of CT states with regard to a distance coordinate, because of the full inclusion of HF exchange, which leads to the cancellation of electron-transfer self-interaction. On the other hand, the excitation energies calculated with CIS or TDHF are usually much too large owing to the calculation of the energies of the virtual orbitals for the $(N + 1)$-electron system instead of for the N-electron system. Therefore, we suggest using a hybrid scheme that combines the benefits of both methods to obtain reasonable estimates for the energies and potential energy surfaces of CT states relative to valence-excited states. This approach can only be seen as a practical

work-around to the CT problem in TDDFT until a more theoretically sound solution is found. However, it is a useful "diagnostic" for whether CT states are in the range of the valence excitations of interest. As the first step of this hybrid approach, a ground-state DFT calculation is performed for the energetically lowest CT state at a large intermolecular distance (R_0) by exchanging the orbital i located at molecule A against the orbital a located at molecule B in the β-part of the wave function. To converge the DFT calculation onto the energetically lowest CT state, we generally use the geometric direct minimization technique (GDM).[151] At shorter distances when the orbitals start to overlap, GDM converges to the closed-shell ground state of the dimer, presumably because the CT solution is no longer a distinct wave function minimum. Otherwise this would provide a convenient way to map out a complete potential energy surface of the CT state. A corrected excitation energy for the lowest CT state is then easily obtained by subtraction of the total energies of the ground state and the CT state, which corresponds to the known ΔDFT method.[152] This excitation energy does not suffer from electron-transfer self-interaction. The self-interaction-free long-range value of the CT excitation energy is then used as a constant offset (for exchange−correlation effects) for the asymptotically correct potential energy curve calculated at the CIS level:

$$\omega_{CT}(R) = \omega_{CT}^{CIS}(R) + (\Delta DFT(R_0) - \omega_{CT}^{CIS}(R_0)) \quad (122)$$

The quality of the total energy of the CT state is roughly the same as the one of the ground state, since the energetically lowest CT state usually corresponds to a pure occupied−virtual single-electron transition over the considered distance range, that is, the excited state is well described by a single Slater determinant. Furthermore, in the limit of the exact xc functional, TDDFT and ΔDFT are equivalent. Plotting the shifted CIS curve together with the curves of the valence-excited states calculated with TDDFT yields a complete self-interaction-free picture of all relevant excited states of the dimer. We have investigated the error that is introduced by using the CIS curve instead of the ΔDFT curve by studying the energetically lowest CT state of a tetrafluoroethylene−ethylene dimer. In this small system, it is possible to converge the ground-state DFT calculation at even shorter distances onto the CT state with the help of a maximum-overlap method (MOM)[153] and thereby to map out a complete potential energy surface for the CT state. We found that by using the CIS curve with the self-interaction-free offset value instead of the ΔSCF curve one introduces an additional error of at most 0.1 eV. Therefore, it can be expected that the accuracy of the hybrid approach for CT states is of about the same order as TDDFT is for valence-excited states.

The proposed hybrid approach is of course not useful for small systems, since more reliable wavefunction-based methods are available, but for large systems, this approach is at present a viable way to gain insight into the energetic positions of intermolecular CT states compared to valence-excited states and to obtain reasonable potential energy curves along an intermolecular separation coordinate. The hybrid approach has already been successfully applied to CT states in large xanthophyll−chlorophyll dimers.[87,111]

In Figure 10, the electron-transfer self-interaction-free PECs of the two energetically lowest CT states of the ZnBC−BC complex are shown that have been calculated along the distance coordinate R with CIS and shifted by a ΔDFT offset. This offset has been calculated for the lowest ZnBC-to-BC CT state to be 3.79 eV and for the lowest BC-to-ZnBC CT state to be 3.95 eV at the level of BLYP/6-31G*. These curves are then plotted together with the curves of the Q-states given by the TDDFT/BLYP/6-31G* calculation. The obtained picture is substantially different from the one obtained by TDDFT alone. First of all, the two energetically lowest CT states are clearly above the valence-excited Q-states of the complex. Second, the CT states do exhibit the correct asymptotic behavior such that the excitation energies do increase with $1/R$. Furthermore, from this picture one can obtain a reasonable value for the lowest intramolecular CT states of the 1,4-phenylene-linked ZnBC−BC complex. At the value of 5.84 Å, the value of R in the full complex, the lowest CT state possesses an excitation energy of 3.75 eV and the second lowest CT state has an excitation energy of 3.91 eV, which agrees with the previously computed lower bound for the excitation energies of these states. Compared with the TDDFT computed values of 1.33 and 1.46 eV for these states, this yields errors in the TDDFT calculation of 2.42 and 2.43 eV, respectively. As a consequence, the spectrum as obtained by TDDFT alone and published previously[142] is an artifact of the approximate xc functionals employed in present-day TDDFT.

6. Brief Summary and Outlook

At present, time-dependent density functional theory (TDDFT) is the most prominent method for the calculation of excited states of medium-sized and large molecules. Every week, a large number of publications appear that present successful applications of the method in fields such as inorganic, organic, and physical chemistry. With the enormous advance in computer technology, systems up to 300 second-row atoms became tractable, which even allows for the treatment of excited-state problems in the fields of biochemistry, biophysics, and material sciences.

TDDFT is a formally exact theory that relies on the analysis of the time-dependent linear response of the formally exact ground-state density to a time-dependent external perturbation, which after Fourier transformation yields exact excited-state energies and oscillator strengths. The derivation of the famous Runge−Gross theorem and the subsequent formulation of a time-dependent Kohn−Sham equation were the cornerstones in the development of the TDDFT formalism. However, since the exact xc functional is not known, approximate xc functionals need to be employed in a practical calculation. Usually the

adiabatic local density approximation (ALDA) is employed, and standard time-independent xc functionals derived for ground-state DFT are used. Concomitantly, errors in the excitation energies and oscillator strengths are introduced. Still, for most valence-excited states, which lie well below the first ionization potential, TDDFT yields results with high accuracy at relatively low computational cost in comparison with highly accurate methods such as MRCI, CASPT2, or EOM-CCSD, which are applicable only to small molecules up to 20 atoms. In fact, the quality of the excitation energies often lies within 0.1−0.5 eV compared with experimental data. Nevertheless, one has to be very careful using TDDFT with approximate xc functionals owing to its failures for Rydberg states, systems with large π-systems, doubly excited states, and CT states. The latter failure limits the applicability of TDDFT to large systems or small molecules in solution or protein environments dramatically, because erroneous inter- and intramolecular CT excited states occur in the low-energy region of the electronic spectra. At present, this prevents TDDFT from being a black-box method for the calculation of excited-state properties in the same fashion that time-independent DFT has become a standard tool for the study of electronic ground states.

In view of these findings, much research is still dedicated to the improvement and development of new xc functionals to eliminate the known failures of TDDFT. However, a remaining open question is whether there exists an approximate xc functional that can describe all excited states equally well. Since different excited states can possess very different electronic structures, it seems unlikely that they can all be captured by one simple approximate xc functional. An approximation may be an excellent one for one class of excited states but at the same time a very poor one for another equally important class of excited states. From this point of view, the discovery of the "one" approximate xc functional that solves all the problems seems unlikely; at least it poses a huge challenge to leading experts in the field.

After its birth in 1984, TDDFT has now left its childhood behind and advanced to a juvenile method that has proven to be a useful alternative approach to standard wave-function-based methods for the calculation of excited states. Whether its indicated failures are remainders of children's diseases that can be fully cured in the future and whether TDDFT thereby possesses the potential to advance to a standard black-box research tool for excited states as its older cousin DFT has become for ground states, the near future will show.

7. Acknowledgments

A. D. gratefully acknowledges financial support by the Deutsche Forschungsgemeinschaft as an "Emmy Noether" fellow. This work was also supported by the Director, Office of Energy Research, Office of Basic Energy Sciences, Chemical Science Division, of the U.S. Department of Energy under Contract No DE-AC03-76SF00098. Computer time has been generously provided by the National Energy Research Scientific Computing Center (NERSC).

8. References

(1) Szabo, A.; Ostlund, N. S. *Modern Quantum Chemistry*; MacMillan Publishing: New York, 1982.
(2) McWeeny, R.; Sutcliffe, B. T. *Methods of Molecular Quantum Mechanics*; Academic Press: London, 1969.
(3) Møller, C.; Plesset, M. S. *Phys. Rev.* **1934**, *46*, 618.
(4) Bartlett, R. J. *Annu. Rev. Phys. Chem.* **1981**, *32*, 359.
(5) Carsky, P. In *Encyclopedia of Computational Chemistry*; Schleyer, P. v. R., Clark, N. L., Gasteiger, J., H. F. S., III, Schreiner, P. R., Eds.; Wiley: Chichester, U.K., 1998; p 485.
(6) Kutzelnigg, W. *J. Mol. Struct. (THEOCHEM)* **1988**, *181*, 33.
(7) Gauss, J. In *Encyclopedia of Computational Chemistry*; Schleyer, P. v. R., Clark, N. L., Gasteiger, J., H. F. S., III, Schreiner, P. R., Eds.; Wiley: Chichester, U.K., 1998; p 615.
(8) Bartlett, R. J., Ed. *Modern Ideas in Coupled-Cluster Methods*; World Scientific: Singapore, 1997.
(9) Parr, R. G.; Yang, W. *Density-Functional Theory of Atoms and Molecules*; Oxford Science Publication: New York, 1989.
(10) Dreizler, R. M.; Gross, E. K. U. *Density functional theory*; Springer-Verlag: Heidelberg, Germany, 1995.
(11) Baerends, E. J.; Gritsenko, O. V. *J. Phys. Chem. A* **1997**, *101*, 5383.
(12) Hohenberg, P.; Kohn, W. *Phys. Rev.* **1964**, *B136*, 864.
(13) Kohn, W.; Sham, L. J. *Phys. Rev.* **1965**, *A140*, 1133.
(14) Buenker, R. J.; Peyerimhoff, S. D.; Butscher, W. *Mol. Phys.* **1978**, *35*, 771.
(15) Buenker, R. J.; Peyerimhoff, S. D.; Bruna, P. J. In *Computational Theoretical Organic Chemistry*; Csizmadia, I. G., Daudel, R., Eds.; Reidel: Dordrecht, The Netherlands, 1981; p 91.
(16) McDonall, J. J.; Peasley, K.; Robb, M. A. *Chem. Phys. Lett.* **1988**, *148*, 183.
(17) Andersson, K.; Malmqvist, P.-Å.; Roos, B. O. *J. Chem. Phys.* **1992**, *96*, 1218.
(18) Roos, B. O. *Adv. Chem. Phys.* **1987**, *69*, 399.
(19) Andersson, K.; Roos, B. O. In *Modern Electronic Structure Theory*; Yarkony, D. R., Ed.; World Scientific: New York, 1995; Vol. 1, p 55.
(20) Emrich, K. *Nucl. Phys. A* **1981**, *351*, 379.
(21) Sekino, H.; Bartlett, R. J. *Int. J. Quantum Chem. Symp.* **1984**, *18*, 255.
(22) Geertsen, J.; Rittby, M.; Bartlett, R. J. *Chem. Phys. Lett.* **1989**, *164*, 57.
(23) Monkhorst, H. J. *Int. J. Quantum Chem. Symp.* **1977**, *11*, 421.
(24) Dalgaard, E.; Monkhorst, H. J. *Phys. Rev. A* **1983**, *28*, 1217.
(25) Koch, H.; Christiansen, O.; Jørgensen, P. *Chem. Phys. Lett.* **1995**, *244*, 75.
(26) Christiansen, O.; Gauss, J.; Schimmelpfennig, B. *Phys. Chem. Chem. Phys.* **2000**, *2*, 965.
(27) Nakatsuji, H.; Hirao, K. *J. Chem. Phys.* **1978**, *68*, 2053.
(28) Gromov, E. V.; Trofimov, A. B.; Vitkovskaja, N. M.; Schirmer, J.; Köppel, H. *J. Chem. Phys.* **2003**, *119*, 737.
(29) Trofimov, A. B.; Stelter, G.; Schirmer, J. *J. Chem. Phys.* **2002**, *117*, 6402.
(30) Schirmer, J. *Phys. Rev. A* **1982**, *26*, 2395.
(31) Head-Gordon, M.; Rico, R. J.; Oumi, M.; Lee, T. J. *Chem. Phys. Lett.* **1994**, *219*, 21.
(32) Head-Gordon, M.; Grana, A. M.; Maurice, D.; White, C. A. *J. Phys. Chem.* **1995**, *99*, 14261.
(33) Christiansen, O.; Koch, H.; Jørgensen, P. *Chem. Phys. Lett.* **1995**, *243*, 409.
(34) Haettig, C.; Weigend, F. *J. Chem. Phys.* **2000**, *113*, 5154.
(35) del Bene, J.; Ditchfield, R.; Pople, J. A. *J. Chem. Phys.* **1971**, *55*, 2236.
(36) Raghavachari, K.; Trucks, G. W.; Pople, J. A.; Head-Gordon, M. *Chem. Phys. Lett.* **1989**, *157*, 479.
(37) Schirmer, J.; Trofimov, A. B. *J. Chem. Phys.* **2004**, *120*, 11449.
(38) Fetter, A. L.; Walecka, J. D. *Quantum Theory of Many-Particle Systems*; McGraw-Hill: New York, 1971.
(39) Runge, E.; Gross, E. K. U. *Phys. Rev. Lett.* **1984**, *52*, 997.
(40) Gross, E. K. U.; Kohn, W. *Phys. Rev. Lett.* **1985**, *55*, 2850.
(41) Gross, E. K. U.; Kohn, W. *Adv. Quantum Chem.* **1990**, *21*, 255.
(42) Casida, M. E. In *Recent Advances in Density Functional Methods, Part I*; Chong, D. P., Ed.; World Scientific: Singapore, 1995; p 155.
(43) van Leeuwen, R. *Int. J. Mod. Phys. B* **2001**, *15*, 1969.
(44) Marques, M. A. L.; Gross, E. K. U. *Annu. Rev. Phys. Chem.* **2004**, *55*, 427.
(45) Foresman, J. B.; Head-Gordon, M.; Pople, J. A.; Frisch, M. J. *J. Phys. Chem.* **1992**, *96*, 135.
(46) Maurice, D.; Head-Gordon, M. *Mol. Phys.* **1999**, *96*, 1533.
(47) Kong, J.; White, C. A.; Krylov, A. I.; Sherrill, D.; Adamson, R. D.; Furlani, T. R.; Lee, M. S.; Lee, A. M.; Gwaltney, S. R.; Adams, T. R.; Ochsenfeld, C.; Gilbert, A. T. B.; Kedziora, G. S.; Rassolov,

V. A.; Maurice, D. R.; Nair, N.; Shao, Y.; Basley, N. A.; Maslen, P. E.; Dombroski, J. P.; Daschel, H.; Zhang, W.; Korambath, P. P.; Baker, J.; Byrd, E. F. C.; Van Voorhis, T.; Oumi, M.; Hirata, S.; Hsu, C.-P.; Ishikawa, N.; Florian, J.; Warshel, A.; Johnson, B. G.; Gill, P. M. W.; Head-Gordon, M.; Pople, J. A. *J. Comput. Chem.* **2000**, *21*, 1532.
(48) CADPAC6: The Cambridge Analytic Derivatives Package Issue 6, Cambridge, England, 1992. A suite of quantum chemistry programs developed by R. D. Amos with contributions from Alberts, I. L.; Andrews, J. S.; Colwell, S. M.; Handy, N. C.; Jayatilaka, D.; Knowles, P. J.; Kobayashi, R.; Koga, N.; Laidig, K. E.; Maslen, P. E.; Murray, C. W.; Rice, J. E.; Sanz, J.; Simandiras, E. D.; Stone, A. J.; Su, M.-D.
(49) Alrichs, R. *TURBOMOLE*, version 5.7.1; University of Karlsruhe: Germany, 2004.
(50) Hirata, S.; Head-Gordon, M.; Bartlett, R. J. *J. Chem. Phys.* **1999**, *111*, 10774.
(51) Stanton, J. F.; Gauss, J.; Ishikawa, N.; Head-Gordon, M. *J. Chem. Phys.* **1995**, *103*, 4160.
(52) Thomas, W. *Naturwissenschaften* **1925**, *13*, 627.
(53) Reiche, F.; Thomas, W. *Z. Phys.* **1925**, *34*, 510.
(54) Kuhn, W. *Z. Phys.* **1925**, *33*, 408.
(55) Davidson, E. R. *J. Comput. Phys.* **1975**, *17*, 87.
(56) Dirac, P. A. M. *Proc. Cambridge Philos. Soc.* **1930**, *26*, 376.
(57) Frenkel, J. *Wave Mechanics, Advanced General Theory*; Clarendon Press: Oxford, U.K., 1934.
(58) Heinrichs, J. *Chem. Phys. Lett.* **1968**, *2*, 315.
(59) Ring, P.; Schuck, P. *The nuclear many-body problem*; Springer-Verlag: Heidelberg, Germany, 1980.
(60) Thouless, D. J. *The Quantum Mechanics of Many Body Systems*; Academic Press: New York, 1972.
(61) Sekino, H.; Bartlett, R. J. *J. Chem. Phys.* **1986**, *85*, 976.
(62) Čížek, J.; Paldus, J. *J. Chem. Phys.* **1967**, *47*, 3976.
(63) McLachlan, A. D.; Ball, M. A. *Rev. Mod. Phys.* **1964**, *36*, 844.
(64) Seeger, R.; Pople, J. A. *J. Chem. Phys.* **1977**, *66*, 3045.
(65) Van Caillie, C.; Amos, R. D. *Chem. Phys. Lett.* **2000**, *317*, 159.
(66) Furche, F.; Ahlrichs, R. *J. Chem. Phys.* **2002**, *117*, 7433.
(67) Eschrig, H. *The Fundamentals of Density Functional Theory*; Teubner Verlag: Stuttgart, Germany, 1996.
(68) Koch, W.; Holthausen, M. C. *A Chemist's Guide to Density Functional Theory*; Wiley-VCH: Weinheim, Germany, 2000.
(69) Baym, G., Ed. *Lecture Notes on Quantum Mechanics*; Perseus Publishing: Cambridge, Massachusetts 1974.
(70) Atkins, P. W. *Molecular Quantum Mechanics*; Oxford University Press: Oxford, U.K., 1983.
(71) van Leeuwen, R. *Phys. Rev. Lett.* **1999**, *82*, 3863.
(72) Yabana, K.; Bertsch, G. F. *Phys. Rev. B* **1996**, *54*, 4484.
(73) Marques, M. A. L.; Castro, A.; Bertsch, G. F.; Rubio, A. *Comput. Phys. Commun.* **2003**, *151*, 60.
(74) Castro, A.; Marquez, M. A. L.; Alonso, J. A.; Bertsch, G. F.; Yabana, K.; Rubio, A. *J. Chem. Phys.* **2002**, *116*, 1930.
(75) Marques, M. A. L.; Lopez, X.; Varsano, D.; Castro, A.; Rubio, A. *Phys. Rev. Lett.* **2003**, *90*, 258101.
(76) Hirata, S.; Head-Gordon, M. *Chem. Phys. Lett.* **1999**, *302*, 375.
(77) Petersilka, M.; Grossmann, U. J.; Gross, E. K. U. *Phys. Rev. Lett.* **1996**, *76*, 1212.
(78) Hirata, S.; Head-Gordon, M. *Chem. Phys. Lett.* **1999**, *314*, 291.
(79) Hsu, C.-P.; Hirata, S.; Head-Gordon, M. *J. Phys. Chem. A* **2001**, *105*, 451.
(80) Becke, A. D. *J. Chem. Phys.* **1993**, *98*, 5648.
(81) Vosko, S. H.; Wilk, L.; Nusair, M. *Can. J. Phys.* **1980**, *58*, 1200.
(82) Becke, A. D. *Phys. Rev. A* **1988**, *38*, 3098.
(83) Lee, C.; Yang, W.; Parr, R. G. *Phys. Rev. B* **1988**, *37*, 785.
(84) Perdew, J. P.; Burke, K.; Enzerhof, M. *Phys. Rev. Lett.* **1996**, *77*, 3865.
(85) Perdew, J. P.; Burke, K.; Enzerhof, M. *Phys. Rev. Lett.* **1997**, *78*, 1396.
(86) Perdew, J. P. *Phys. Rev. B* **1986**, *33*, 8822.
(87) Dreuw, A.; Fleming, G. R.; Head-Gordon, M. *Phys. Chem. Chem. Phys.* **2003**, *5*, 3247.
(88) Dunietz, B. D.; Dreuw, A.; Head-Gordon, M. *J. Phys. Chem. B* **2003**, *107*, 5623.
(89) Becke, A. D. *J. Chem. Phys.* **1988**, *88*, 2547.
(90) Olsen, J.; Jørgen, H.; Jensen, A.; Jørgensen, P. *J. Comput. Phys.* **1988**, *74*, 265.
(91) Eichkorn, K.; Treutler, O.; Öhm, H.; Häser, M.; R, A. *Chem. Phys. Lett.* **1995**, *240*, 283.
(92) Jamorski, C.; Casida, M. E.; Salahub, D. R. *J. Chem. Phys.* **1996**, *104*, 5134.
(93) Bauernschmitt, R.; Häser, M.; Treutler, O.; Ahlrichs, R. *Chem. Phys. Lett.* **1997**, *264*, 573.
(94) Savin, A.; Umrigar, C. J.; Gonze, X. *Chem. Phys. Lett.* **1998**, *288*, 391.
(95) Gritsenko, O.; Baerends, E. J. *J. Chem. Phys.* **2004**, *121*, 655.
(96) Cai, Z.-L.; Sendt, K.; Reimers, J. R. *J. Chem. Phys.* **2002**, *117*, 5543.
(97) Grimme, S.; Parac, M. *Chem. Phys. Chem.* **2003**, *3*, 292.
(98) Cave, R. J.; Zhang, F.; Maitra, N. T.; Burke, K. *Chem. Phys. Lett.* **2004**, *389*, 39.
(99) Maitra, N. T.; Zhang, F.; Cave, R. J.; Burke, K. *J. Chem. Phys.* **2004**, *120*, 5932.
(100) Tozer, D. J.; Amos, R. D.; Handy, N. C.; Roos, B. J.; Serrano-Andres, L. *Mol. Phys.* **1999**, *97*, 859.
(101) Dreuw, A.; Weisman, J. L.; Head-Gordon, M. *J. Chem. Phys.* **2003**, *119*, 2943.
(102) Dreuw, A.; Head-Gordon, M. *J. Am. Chem. Soc.* **2004**, *126*, 4007.
(103) Sobolewski, A. L.; Domcke, W. *Chem. Phys.* **2003**, *294*, 73.
(104) van Leeuwen, R.; Baerends, E. J. *Phys. Rev. A* **1994**, *49*, 2421.
(105) Grüning, M.; Gritsenko, O. V.; van Gisbergen, S. J. A.; Baerends, E. J. *J. Chem. Phys.* **2001**, *114*, 652.
(106) Görling, A. *Phys. Rev. Lett.* **1999**, *83*, 5459.
(107) Ivanov, S.; Hirata, S.; Bartlett, R. J. *Phys. Rev. Lett.* **1999**, *83*, 5455.
(108) Della Sala, F.; Görling, A. *Int. J. Quantum Chem.* **2002**, *91*, 131.
(109) Pople, J. A.; Binkley, J. S.; Seeger, R. *Int. J. Quantum Chem. Symp.* **1976**, *10*, 1.
(110) Van Caillie, C.; Amos, R. D. *Chem. Phys. Lett.* **1999**, *308*, 249.
(111) Dreuw, A.; Fleming, G. R.; Head-Gordon, M. *J. Phys. Chem. B* **2003**, *107*, 6500.
(112) Tozer, D. J. *J. Chem. Phys.* **2005**, *119*, 12697.
(113) Perdew, J. P.; Parr, R. G.; Levy, M.; Balduz, J. L., Jr. *Phys. Rev. Lett.* **1982**, *49*, 1691.
(114) Tawada, Y.; Tsuneda, T.; Yanagisawa, S.; Yanai, T.; Hirao, K. *J. Chem. Phys.* **2004**, *1210*, 8425.
(115) Yanai, T.; Tew, D. P.; Handy, N. C. *Chem. Phys. Lett.* **2004**, *393*, 51.
(116) Baer, R.; Neuhauser, D. *Phys. Rev. Lett.* **2005**, *94*, 043002.
(117) Stoll, H.; Savin, A. In *Density Functional Methods in Physics*; Dreizler, R. M., da Providencia, J., Eds.; Plenum: New York, 1985; p 177.
(118) Savin, A. In *Recent Developments and Applications of Modern Density Functional Theory*; Seminario, J. M., Ed.; Elsevier: Amsterdam, 1996.
(119) Leininger, T.; Stoll, H.; Werner, H.-J.; Savin, A. *Chem. Phys. Lett.* **1997**, *275*, 151.
(120) Iikura, H.; Tsuneda, T.; Yanai, T.; Hirao, K. *J. Chem. Phys.* **2001**, *115*, 5340.
(121) van Faassen, M.; de Boeij, P. L.; van Leeuwen, R.; Berger, J. A.; Snijders, J. G. *J. Chem. Phys.* **2003**, *118*, 1044.
(122) Baerends, E. J.; Autschbach, J.; Brces, A.; Bo, C.; Boerrigter, P. M.; Cavallo, L.; Chong, D. P.; Deng, L.; Dickson, R. M.; Ellis, D. E.; Fan, L.; Fischer, T. H.; Fonseca Guerra, C.; van Gisbergen, S. J. A.; Groeneveld, J. A.; Gritsenko, O. V.; Grning, M.; Harris, F. E.; van den Hoek, P.; Jacobsen, H.; van Kessel, G.; Kootstra, F.; van Lenthe, E.; McCormack, D. A.; Osinga, V. P.; Patchkovskii, S.; Philipsen, P. H. T.; Post, D.; Pye, C. C.; Ravenek, W.; Ros, P.; Schipper, P. R. T.; Schreckenbach, G.; Snijders, J. G.; Sola, M.; Swart, M.; Swerhone, D.; te Velde, G.; Vernooijs, P.; Versluis, L.; Visser, O.; van Wezenbeek, E.; Wiesenekker, G.; Wolff, S. K.; Woo, T. K.; Ziegler, T. *ADF2004.01, SCM, Theoretical Chemistry*; Vrije Universiteit: Amsterdam, The Netherlands, http://www.scm.com.
(123) Martin, R. L. *J. Chem. Phys.* **2003**, *118*, 4775.
(124) Amos, A. T.; Hall, G. G. *Proc. R. Soc. A* **1961**, *263*, 483.
(125) Batista, E. R.; Martin, R. L. *J. Phys. Chem. A* **2005**, *109*, 3128.
(126) Clark, A. E.; Martin, R. L.; Hay, P. J.; Green, J. C.; Jantunen, K. C.; Kiplinger, J. L. *J. Phys. Chem. A* **2005**, *109*, 5481.
(127) Climent, T.; Gonzalez-Luque, R.; Merchan, M. *J. Phys. Chem. A* **2003**, *107*, 6995.
(128) Serrano-Andres, L.; Merchan, M.; Jablonski, M. *J. Chem. Phys.* **2003**, *119*, 4294.
(129) Molina, V.; Merchan, M. *J. Phys. Chem. A* **2001**, *105*, 3745.
(130) Wiberg, K. B.; Hadad, C. M.; Foresman, J. B.; Chupka, W. A. *J. Phys. Chem.* **1992**, *96*, 10756.
(131) Grana, A. M.; Lee, T. J.; Head-Gordon, M. *J. Phys. Chem.* **1995**, *99*, 3493.
(132) Halasinski, T. M.; Weisman, J. L.; Ruiterkamp, R.; Lee, T. J.; Salama, F.; Head-Gordon, M. *J. Phys. Chem. A* **2003**, *107*, 3660.
(133) Vaswani, H. M.; Hsu, C. P.; Head-Gordon, M.; Fleming, G. R. *J. Phys. Chem. B* **2003**, *107*, 7940.
(134) Weisman, J. L.; Head-Gordon, M. *J. Am. Chem. Soc.* **2001**, *123*, 11686.
(135) Oumi, M.; Maurice, D.; Head-Gordon, M. *Spectrochim. Acta A* **1999**, *55*, 525.
(136) Franzen, S.; Kiger, L.; Poyart, C.; Martin, J.-L. *Biophys. J.* **2001**, *80*, 2372.
(137) Dreuw, A.; Dunietz, B. D.; Head-Gordon, M. *J. Am. Chem. Soc.* **2002**, *124*, 12070.
(138) Derewenda, Z.; Dodson, G.; Emsley, P.; Harris, D.; Nagai, K.; Perutz, M.; Reynaud, J.-P. *J. Mol. Biol.* **1990**, *211*, 515.
(139) Della Longa, S.; Arcovito, A.; Girasole, M.; Hazemann, J. L.; Benfatto, M. *Phys. Rev. Lett.* **2001**, *87*, 155501.
(140) Makinen, M. W.; Eaton, W. *Ann. N. Y. Acad. Sci.* **1973**, *206*, 210.
(141) Yamaguchi, Y.; Yokomichi, Y.; Yokoyama, S.; Mashiko, S. *Int. J. Quantum Chem.* **2001**, *84*, 338.
(142) Yamaguchi, Y.; Yokoyama, S.; Mashiko, S. *J. Chem. Phys.* **2002**, *116*, 6541.

(143) Miyahara, T.; Nakatsuji, H.; Hasegawa, J.; Osuka, A.; Aratani, N.; Tsuda, A. *J. Chem. Phys.* **2002**, *117*, 11196.
(144) Cho, H. S.; Jeong, D. H.; Yoon, M.-C.; Kim, Y. H.; Kim, Y.-R.; Kim, D.; Jeoung, S. C.; Kim, S. K.; Aratani, N.; Shinmori, H.; Osuka, A. *J. Phys. Chem. A* **2001**, *105*, 4200.
(145) Häberle, T.; Hirsch, J.; Pöllinger, F.; Heitele, H.; Michel-Beyerle, M. E.; Anders, C.; Döhling, A.; Krieger, C.; Rückemann, A.; Staab, H. A. *J. Phys. Chem.* **1996**, *100*, 18269.
(146) Polivka, T.; Zigmantas, D.; Herek, J. L.; He, Z.; Pascher, T.; Pulleritis, T.; Cogdell, R. J.; Frank, H. A.; Sundström, V. *J. Phys. Chem. B* **2002**, *106*, 11016.
(147) Thomson, M.; Novosel, M.; Roskos, H. G.; Müller, T.; Wagner, M.; Fabrizi de Biani, F.; Zanello, P. *J. Phys. Chem. A* **2004**, *108*, 3281.
(148) Hasegawa, J.; Ozeki, Y.; Ohkawa, K.; Hada, M.; Nakatsuji, H. *J. Phys. Chem. B* **1998**, *102*, 1320.
(149) Hashimoto, T.; Choe, Y. K.; Nakano, H.; Hirao, K. *J. Phys. Chem. A* **1999**, *103*, 1894.
(150) Parusel, A. B. J.; Grimme, S. *J. Porphyrins Phthalocyanines* **2001**, *5*, 225.
(151) Voorhis, T. V.; Head-Gordon, M. *Mol. Phys.* **2002**, *100*, 1713.
(152) Ziegler, T.; Rauk, A.; Baerends, E. J. *Theor. Chim. Acta* **1977**, *43*, 261.
(153) Gilbert, A. T. B.; Gill, G. B. W.; Gill, P. M. W., manuscript in preparation.
(154) Vasudevan, J.; Stibrany, R. T.; Bumby, J.; Knapp, S.; Potenza, J. A.; Emge, T. J.; Schugar, H. J. *J. Am. Chem. Soc.* **1996**, *118*, 11676.
(155) Scheer, H.; Inhoffen, H. H. In *The Porphyrins*; Dolphin, D., Ed.; Academic: New York, 1978; Vol. 2, p 45.

CR0505627